

“RECONFIGURABLE MOLD FOR
CUSTOM TEXTILE COMPOSITE FACADE
PANELS”

A Thesis

Presented to the Faculty

of Philadelphia University

in Partial Fulfillment of the Requirements for the Degree of

Master of Science in Textile Engineering

by

Satpal Singh Gurjar

December 2017

©2017 Satpal Singh Gurjar

ABSTRACT

Composite materials offer an appealing combination of low weight and high strength that is especially sought after in high-performance applications. The use of composite materials has and is continuing to increase, and the use of the material has been shown to provide substantial weight savings in, for example, spacecraft, aircraft, and skyscraper designs. With the increased use of composite materials follows increased demand for cost-efficient manufacturing methods. Composite products are in many cases manufactured either by manual operations or using complex automated solutions associated with high investment costs. The objective of this research is to explore an approach to develop an automated reconfigurable prototype for fabrication of textile reinforced composites and perform the manufacturing of different samples to prove the proposed prototype concept. This prototype is a mock-up that links the design of geometrically of complex facade panels to a reconfigurable mold system. This research provides the opportunity to understand essential parameters of a digitally controlled reconfigurable mold system which supports the fabrication of geometrically complex textile reinforced facade panels.

The research was sponsored by the MAG COMPOSITES CENTER and the Architecture Program at Jefferson (Philadelphia University + Thomas Jefferson University). Because of this flexible mold prototype method, we have fabricated many physical samples which are used to show that off-the-shelf solutions can be used to digitally control a flexible mold prototype to manufacture textile composite panels. The advantage of this research is that we can reduce the high cost associated with making custom molds for non-repetitive free-form composite panel surfaces. The research also highlights the limitations of the developed prototype such as the limitations of surface curvatures that can be achieved with the proposed actuator

system and mold surface, and panel boundary conditions. With this approach, my perspective is to find solutions that are compatible and easy to adopt with the entire manufacturing system, which is an economic need for repeating multiple identical and unique structures by removing of expensive formwork or another tooling in mold making process

ACKNOWLEDGEMENTS

I am grateful to my advisor, Dr. Brian George, Ph.D., for his constant and sincere attention. I am deeply indebted to Dr. Kihong Ku for his kind guidance and assistance in the experimental stage. I would also like to express my gratitude to Raymond Lucia for his assistance in understanding the electronics involved and an equally supportive hand in this project. I would also like to thank Mr. Trevor, DEC Technical Shop Associate, Philadelphia University + Thomas Jefferson, for allowing us to use the equipment of the DEC shop facility. Last but not least, I am happy to convey my deep appreciation to my parents who selflessly supported me for this unbelievable journey to the United States of America.

Table of Contents

Abstract	iii
Table of Contents	vi
List of Figures	viii
1. Introduction	1
1.1 Architecture Freeform Facade Structures	1
1.2 Objectives and Scope of the Study	3
2. Architectural Examples of Freeform Structures	4
2.1 Introduction	4
2.2 Architectural Structures Using Curvatures:	5
2.3 Discussion	6
3. Present Formwork Technology and its Limitations	8
3.1 Introduction	8
3.2 Available Techniques for Free Form Composite Surface	8
3.3 Discussion of Available Techniques	9
4. Introduction of Composites	11
4.1 Materials	12
Fibers:	12
Fabric:	12
4.2 Matrices	15
4.2.1 Epoxy Resin	15
4.2.2 Cure Agent	18
5. Literature On Reconfigurable Mold Techniques	19
5.1 Introduction	19
5.2 Conventional Semi-Automatic Mold Techniques:	20
5.3 Contemporary Molding Techniques:	27
5.4 Conclusion	34
6. Experimentation and Prototyping	37
6.1 Preliminary Phases of the Mold Prototype Development	38
6.1.1 Static Mold	38
6.1.2 Movable Surface Mold Using Pin Bed Concept	41
6.2 Stage I: Proposed Prototype Method	43
6.2.1 First Step: Digital to Physical Actuation	43
6.2.2 Second Step: Construction of Prototype Body	44
6.2.3 Stage Ii: Production Process of Composite Architectural Panel	48
6.2.4 Step 4 – Final Sample Testing and Analysis by Rhino and Auto Desk Alia 52	

6.3 Results and Discussion.....	70
7. Conclusion.....	77
8. Recommendations for Further Research	79
9. References	80
Appendix A.....	83
Appendix B.....	88
Appendix C.....	92
Appendix D	95
Appendix E.....	97

LIST OF FIGURES

Figure 1.1. Example of Fiberglass fabricated panel structure: The House of Dior in Seoul, South Korea, designed by Christian de Portzamparc delivered in June 2015 (Portzamparc).....	2
Figure 4.1. Classification of Raw Material (Mazumdar).....	12
Figure 4.2. Chemical Structure of ethoxylene group (Compiled in draw.io)	16
Figure 4.3 Chemical Structure of glycidyl group (Compiled in draw.io).....	16
Figure 4.4. Chemical Reaction (Reinhart et al.)	17
Figure 4.5. Homopolymerization of epoxide (Compiled in draw.io)	17
Figure 5.1. Pneumatic form-finding method (Bechthold).....	20
Figure 5.2. Morphological study of a pavilion in glass-fiber reinforced plastic, source: Piano [1969] (Schipper).....	22
Figure 5.3. Pavilion made out of triangular double-curved plastic panels, source: Piano [1969] (Schipper).....	22
Figure 5.4. “Stampo Deformabile” or “Deformable Mold” from Renzo Piano, source: Piano [1969] (Schipper).....	23
Figure 5.5. Structure of the experimental device for a press working (Nakajima).....	24
Figure 5.6. Variable Configuration Mold Thermoforming (Kleespies and Crawford).	26
Figure 5.7. Optimum forming and multi-point deformation (Boers).....	28
Figure 5.8. A discrete approximation to a continuous surface (Dhande and Rao). ...	29
Figure 5.9. Flex-Rod’ (Rietbergen and Vollers).	30
Figure 5.10. The mold attached to Injection molding method (Rooy et al.).....	31
Figure 5.11. Multipoint stretch forming machine: (a) medium-scale computerized multipoint stretch forming machine; (b) mildly curved panels are fabricated using	

two-way stretch forming only; (c) complex shapes are pressed once more with the upper multipoint forming mold; (d) the curved panels are cut and perforated with a special computerized laser-cutting machine (Lee and Kim).....32

Figure 5.12. a) In left Casting hot wax in mold and b) right Formed wax element on the mold (Oesterle).33

Figure 5.13. Handling procedures for 2-sided formwork on-site: 1. placement of the support structure side a; 2. attaching of wax elements, tie rods and form ties; 3. assembly of side b; 4. attaching side a and b. (Oesterle)34

Figure 6.1 Curved Panel formation on Static Mold a) Wooden board CNC milled mold b) Hand lay-up of composite materials and matrix c) Final free form double curved panel d) Final free form double curved surface (Pictures courtesy Gurjar).....40

Figure 6.2 a) Pin bed shelf and b) game (Rogers).41

Figure 6.3 Process of curved panel formation by pin bed method a) Pin bed frame, b) CNC molded shape, c) Pin bed with curved structure, d) Composite layup, e) Drying Panel, f) Finished panel (Pictures courtesy Gurjar).....42

Figure 6.4 Design of panel on a) Rhino and b) Firefly Plugin script for shift register (Ku).....43

Figure 6.5. Drawing of Prototype Design a) open and b) closed (Drawn by Gurjar). 45

Figure 6.6 Prototype Mold assembly with Silicon flexible membrane attachment with vertical actuators (Ku).....46

Figure 6.7. Top flexible silicon rubber membrane (Picture courtesy Gurjar).....46

Figure 6.8. Arduino Microcontroller (Picture courtesy Gurjar).....47

Figure 6.9. Actuator Matrix a) Actuators assembly and b) Actuators inside assembly (Picture courtesy Gurjar).....47

Figure 6.10. Male spring Top (Picture courtesy Gurjar).....48

Figure 6.11. Prototype Mold (Picture courtesy Gurjar).....	48
Figure 6.12 Production process of composite Architectural Panel a) Material Preparation b) Actuators and flexible membrane setting c) Actuators in motion d) Material Layup process e) Vacuum Bagging f) Vacuum processing g) Cured Composite panel h) Finished composite panel (Picture courtesy Gurjar)	51
Figure 6.13 3-D Digital Evaluation (Ku).....	52
Figure 6.14. Double Curve Analysis using Rhino and Alias Auto Desk a) Double Curved front view b) Double Curved Side view, c) Cross sectional view, d) Rhino 3D structure, e) Scan sample in Rhino, f) Evaluation of scanned sample with ideal 3D structure. (Pictures courtesy Gurjar).....	53
Figure 6.15. Double Curve Analysis using Rhino and Alias Auto Desk a) Double Curved front view b) Double Curved Side view, c) Cross sectional view, d) Rhino 3D structure, e) Scan sample in Rhino, f) Evaluation of scanned sample with ideal 3D structure. (Pictures courtesy Gurjar)	55
Figure 6.16. Double Curve Analysis using Rhino and Alias Auto Desk a) Double Curved front view b) Double Curved Side view, c) Cross sectional view, d) Rhino 3D structure, e) Scan sample in Rhino, f) Evaluation of scanned sample with ideal 3D structure. (Pictures courtesy Gurjar).....	56
Figure 6.17. Concave Curve Analysis using Rhino and Alias Auto Desk a) Concave Curved front view b) Concave Curved Side view, c) Cross sectional view, d) Rhino 3D structure, e) Scan sample in Rhino, f) Evaluation of scanned sample with ideal 3D structure. (Pictures courtesy Gurjar).....	58
Figure 6.18. Concave Curve Analysis using Rhino and Alias Auto Desk a) Concave Curved front view b) Concave Curved Side view, c) Cross sectional view, d) Rhino	

3D structure, e) Scan sample in Rhino, f) Evaluation of scanned sample with ideal 3D structure. (Pictures courtesy Gurjar)59

Figure 6.19. Concave Curve Analysis using Rhino and Alias Auto Desk a) Concave Curved front view b) Concave Curved Side view, c) Cross sectional view, d) Rhino 3D structure, e) Scan sample in Rhino, f) Evaluation of scanned sample with ideal 3D structure. (Pictures courtesy Gurjar)60

Figure 6.20. Convex Curve Analysis using Rhino and Alias Auto Desk a) Convex Curved front view b) Convex Curved Side view c) Convex Curved Back view d) Side View, e) Rhino 3D structure, f) Scan sample in Rhino, g) Evaluation of scanned sample with ideal 3D structure. (Pictures courtesy Gurjar)62

Figure 6.21. Convex Curve Analysis using Rhino and Alias Auto Desk a) Convex Curved front view b) Convex Curved Back view c) Convex Curved Side view d) Rhino 3D structure, e) Scan sample in Rhino, f) Evaluation of scanned sample with ideal 3D structure. (Pictures courtesy Gurjar)63

Figure 6.22. Convex Curve Analysis using Rhino and Alias Auto Desk a) Convex Curved front view b) Convex Curved Back view c) Convex Curved Side view d) Rhino 3D structure, e) Scan sample in Rhino, f) Evaluation of scanned sample with ideal 3D structure. (Pictures courtesy Gurjar)65

Figure 6.23. Freeform Curve Analysis using Rhino and Alias Auto Desk a) Freeform front view b) Freeform Side view c) Freeform cross section view d) Rhino 3D structure, e) Scan sample in Rhino, f) Evaluation of scanned sample with ideal 3D structure. (Pictures courtesy Gurjar)66

Figure 6.24. Freeform Curve Analysis using Rhino and Alias Auto Desk a) Freeform front view b) Freeform Side view c) Freeform cross section view d) Rhino 3D

structure, e) Scan sample in Rhino, f) Evaluation of scanned sample with ideal 3D structure. (Pictures courtesy Gurjar)	68
Figure 6.25. Freeform Curve Analysis using Rhino and Alias Auto Desk a) Freeform front view b) Freeform Side view c) Freeform cross section view d) Rhino 3D structure, e) Scan sample in Rhino, f) Evaluation of scanned sample with ideal 3D structure. (Pictures courtesy Gurjar)	69
Figure 6.26. Double curve geometry comparison of ideal versus actual at individual actuator.....	71
Figure 6.27. Concave curve geometry comparison of ideal versus actual at individual actuator.....	72
Figure 6.28. Convex curve geometry comparison of ideal versus actual at individual actuator.....	73
Figure 6.29. Freeform curve geometry comparison of ideal versus actual at individual actuator.....	74
Figure 6.30. Double Curved Normality Graph for higher values. ... Error! Bookmark not defined.	
Figure 6.31. Double Curved Normality Graph for Lower values. ... Error! Bookmark not defined.	
Figure 6.32. Concave Curved Normality Graph for higher values. . Error! Bookmark not defined.	
Figure 6.33. Concave Curved Normality Graph for lower values. ... Error! Bookmark not defined.	
Figure 6.34. Convex Shape Normality Graph for higher values. Error! Bookmark not defined.	

Figure 6.35. Convex Shape Normality Graph for lower values.**Error! Bookmark not defined.**

Figure 6.36. Freeform Structure Normality Graph for higher values. **Error! Bookmark not defined.**

Figure 6.37. Freeform Structure Normality Graph for lower values. **Error! Bookmark not defined.**

LIST OF TABLES

Table 1. Freeform architectural Structure examples	5
Table 2.1. Glass fiber Composition (Reinhart et al.)	14
Table 3. Inherent properties of glass fibers (Reinhart et al.).....	14
Table 4. Different mold techniques.....	34
Table 5. Double curved height comparison between ideal and actual samples	88
Table 6. Concave Curve height comparison between ideal and actual samples	89
Table 7. Convex curve height comparison between ideal and actual samples	89
Table 8. Freeform Curve height comparison between ideal and actual samples	90

1. INTRODUCTION

1.1 Architecture Freeform Facade Structures

During the last decade, digital technology has undergone tremendous improvement in the field of architecture. It provides prominent geometric complexity in design and engineering field (Daan Rietbergen). Software like Rhinoceros, Revit, and AutoCAD rule the architecture world allowing the design of more complex forms. However, such geometrical complex elements create challenges for the manufacturing industry, making the transition to physical realization is challenging and expensive. The conventional molding method forced designers to simplify complex shape buildings. The facade of prestigious buildings like Kunsthau in Graz was produced using expensive molding techniques where every part of the facade must be produced using a unique mold (Pronk et al.). Computer-aided designs are driving new approaches for constructing complex folded and curved shapes with the required precision. Emerging approaches include pneumatic or hanging fabric formwork, the use of high-speed CNC (Computerized Numerical Control) milling to shape foam sandwich cores and concrete formwork, as well as origami-like strategies to create overall complexity using simple, planar elements that vary in size. However, the constraints of components with large curvatures, make the process especially suited for larger, double-curved surfaces like facades or walls, where the curvature of each element is relatively small in comparison to the overall shape. This provides a pressing necessity to develop a flexible molding technique that is economically attractive and is not only limited to architecture but can be applied to other fields like the automotive industry and aerospace industry (Bechthold).

Architectural systems depend on the combination of different structures to form large facades. Using the composite structure, Christian de Portzamparc delivered an impressive freeform structure design. As illustrated in Figure 1.1 below, his building has volutes of the facade executed as boat hulls, made with fiberglass reinforced composite, with impressive size. The panels, more than twenty meters high and seven meters wide, are designed in one piece, are textured, and reproduce the pattern of weaving on The House of Dior building (Portzamparc).



Figure 1.1. Example of Fiberglass fabricated panel structure: The House of Dior in Seoul, South

The fundamental concept of the work presented here is not limited to the new approaches of construction and fabrication, but also to the development of high-performance materials, which present unprecedented opportunities in design, and construction.

1.2. Objectives and scope of the study

Research focuses on the development of the flexible automated mold and the link between the geometrical framework of the flexible mold systems and the application and fabrication of the textile composites. The research provides the opportunity to develop complex curved geometries following predefined structural and morphological requirements of the architectural designers.

The goals of this research are as follows:

1. Develop a reconfigurable mold prototype.
2. Prove the proof of concept by manufacturing different shapes of panels.
 - a. Samples are repeatable
 - b. Samples are same as ideal 3-D design.

2. ARCHITECTURAL EXAMPLES OF FREEFORM STRUCTURES

2.1 Introduction

This chapter presents various architecture examples and cases or architectural designs. These architectural designs are analyzed based on following factors – geometrical aspects, curvature, type of elements and potential to apply the flexible mold method in different architectural structures (Bechthold).

Simple things sometimes turn out to be highly complex and challenging. The hardest line to draw by hand is a perfectly straight line. Architects spend long nights spend long nights staring at computer screens and models to fine-tune the proportions and details of their minimalist schemes. In the domain of structures, similar principles hold with the design of the simplest of all the structural systems – a curved or folded surface. Lured by the seeming simplicity of this concept, generations of architects joyfully designed intricate surfaces using physical and, lately digital models.





Eventually, many find out that, unfortunately, the form is not suitable to carry loads, at least not as designed as designed and with the support to carry loads, at least not as designed and with the supports and proposed edge conditions. These types of discoveries have become even more frequent as digital models of highly complex surfaces are now easily produced with powerful computer-aided design (CAD) surface modelers (Bechthold).




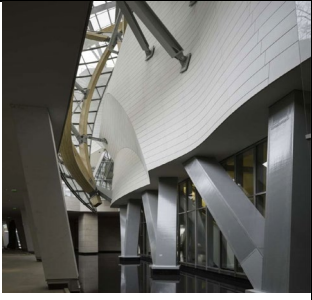

Structural surfaces include tensile membranes, shells and folded plates, systems that can be highly efficient if designed based on their underlying structural principles, and equally problematic if poorly understood. These systems derive their stiffness from folds or curvature and, in the case of membranes, pre-stressing. Also new materials such as fluoropolymer films, for example, are now introduced into construction and broaden design scope in unprecedented ways. Curved or folded rigid surfaces are

being built again, facilitated by state-of-the-art structural optimization and simulation tools and innovative construction techniques. Over the past decades, significant impulses for the design and construction of structural surfaces have come from developments of cutting-edge digital design techniques, new material technologies, and powerful computer-numerically controlled (CNC) manufacturing methods. (Bechthold)

2.2 Architectural Structures Using Curvatures:

Table 1. Freeform architectural Structure examples

Year	Project title, city, country (architect/ structural engineer)	Type of structure and Material used	Image
1933	Algeciras, Spain (arch. Manuel S´anchez Arcas / s.e. Eduardo Torroja)	Thin concrete shell dome, Diameter 47.6 m; thickness 10+ cm (Torroja).	
1962	Trans World Airlines (TWA) Terminal, JFK Airport, New York, N.Y., United States (arch. Eero Saarinen and Associates)	Freeform structure, Aluminium panel and fiber reinforced concrete. (Casillas, Mellow and Miller).	
1974	St. Joseph’s Hospital, United States (arch. Bertrand Goldberg, Tacoma, Wash.,)	Tubular structure, Made of reinforced concrete (St. Joseph’s Hospital).	
1978	‘The Egg’ Center for the Performing Arts, Albany, N.Y., United States (arch. Wallace Harrison)	Curved structure, Modern architecture (The Egg).	

1986	Lotus Temple, New Delhi, India (arch. Fariborz Sahba / s.e. Flint & Neill)	Concrete frame and precast concrete ribbed roof (Sahba).	
1996	Grand Central Water Tower, South Africa (arch. GAPP Architects & Urban Designers)	Inverted conical container made of concrete (Muwanga).	
2006	Mercedes Benz Museum, Stuttgart, Germany (UN studio)	Freeform structure, Made of precast metal sheet panels (Mercedes-Benz).	
2014	Fondation Louis Vuitton pour la Creation (arch. Frank ' Gehry, s.e. RFR)	curved FRC tile cladding, by use of rubber moulds on EPS formwork. (Gehry).	
2015	The House of Dior in Seoul, South Korea, designed by Christian de Portzamparc	Freeform structure, Panels made up of Fibre Glass Composite (Portzamparc).	

2.3 Discussion

The curved architecture has a very long history. The traditional method of constructing concrete shell is a tedious and lengthy process. This process involved using CNC milled wood, steel formwork which makes process restrict to reusability of the molds.

Keeping the above-stated examples in view, the current trend in architectural projects demand using various free-form structures for unique forms and aesthetic reasons. It concludes that a manufacturing method is required which can develop light weighted panels, floors, and other curved and freeform structures. It created insight into the type of architecture that could benefit from a production method using a flexible mold with the help of 3D software facilitating the design and randomized shapes of the free-form architecture structures.

3. PRESENT FORMWORK TECHNOLOGY AND ITS LIMITATIONS

3.1 Introduction

For construction applications, the thinness and complex geometry of the rigid structure is a big challenge. Current methods and techniques of building freeform structure is a challenge when the structure is a 3-Dimensional form. A high cost has been associated with making a curved or intricately folded surface and has led to an economic need for repeating multiple identical systems to spread the cost of expensive formwork or another tooling. Cost and the need for repetition is often a limitation that excludes the use of rigid structural surfaces altogether (Bechthold).

In architectural construction, a primary concern is to keep the costs for molds as low as possible. Mold is a major component of forming a structure. Mold making is a low-volume production technique, but it is limited to large curved surfaces. Other than handmade mold techniques, CNC milling machines that carve foam molds made the process less complex for the mold making process (Bechthold).

3.2 Available Techniques for Free Form Composite Surface

1. CNC foam milling
2. Timber Molds
3. Steel Molds
4. Rubber Molds
5. Thermoplastic Molds
6. Clay Molds

Preferred molding techniques is divided into these different categories:

- 1) **The static mold:** This is the most common mold technique made of polyurethane/polystyrene, wood, metal alloys which can be 3D formed by CNC cutting machine. However, this technique is not efficient as it produces a

lot of waste. Also, it restricts the reusability of the mold. For example, CNC foam milled mold, timber molds, steel molds, vacuum and air pressure forming, wire cutting, etc (Pronk et al.).

- 2) **The reusable mold:** Reusable molds are made of clay or wax. Reusability makes the process environmentally friendly and creates less waste. It is labor intensive and can be reusable. Eg. Clay mold, Wax mold (Pronk et al.).
- 3) **The flexible mold:** In this molding method we can create varying shapes of elements for whole structure and assemble them in the desired structure. Examples of this kind of mold are the Flexi Mold by Boers, and the adjustable mold by Rietbergen & Vollers. The mold contains a field of height-adjustable pins, and individual pin can be set into height using a computer-automated machine. The pins are covered with a polymer sheet to create a smooth surface. It is essential to avoid that the pins give a local distortion of the surface. The downside of these flexible molds is the high investment and still requires many developments to get a perfect structural surface (Pronk et al.).

3.3 Discussion of available techniques

In freeform construction, it would be typical for the mold to shape the visible interior surface with the best shape and finish. In recent days innovations have not been limited to new approaches to construction and fabrication. Conventionally built environment mainly consists of Flat shapes, and therefore the formworks also contain flat panels but exciting developments in high-performance materials present unprecedented opportunities in the design and construction of rigid structural surfaces. Glass technology, ultra-high-strength fiber concrete, and polymer composites, for example, are only beginning to be introduced in architecture. Recent

development in computer-aided design, engineering, and manufacturing are opening new approaches to constructing complex folded and curved shapes with the required precision. CAD/CAM and CNC technology enabled efficient translation of digital form into physical shape and structure while expensive processes of mold making necessitated the application automation and reusability in the field of Adjustable molds and complex structures forming.

4. INTRODUCTION OF COMPOSITES

A composite material is an amalgamation of two or more materials that results in highly efficient properties than the individual materials used alone. The main advantages of composite materials are their high strength and stiffness, combined with low density, when compared with bulk materials, allowing for a weight reduction in the finished part (Campbell). Composite materials offer vast potential in the application of architecture specifically due to the high strength to weight ratio, where the material properties are adjusted according to mechanical and aesthetic demands through lamination and additives. The low thermal conductivity makes composite materials suitable for use as structural elements and building envelopes (Corazza et al.). Matrices for use with these fibers are mostly thermosetting polyesters and epoxies. Polyesters are less expensive but are mechanically inferior to most epoxies. Both can be formulated to cure at room temperature under moderate pressures. Most fabrication processes applicable to architectural components utilize the resins in liquid form for the wetting of the fibers (Bechthold).

The two constituents of composite materials are reinforcement and a matrix. The reinforcement provides the strength and structure. The matrix distributes the loads to the high strength fibers, prevents them from buckling and helps to maintain their position in the system. Fibers typically are short discontinuous elements which can be produced into mats and scrims, or else long yards, configured into woven or unidirectional mats or processed in special rotational manufacturing processes (Bechthold). Typical fiber materials suitable for use in architectural construction include glass, carbon and aramid fibers (as shown in Figure 4.1). Among these materials, glass is comparatively inexpensive. The driving force for the use of glass- and carbon-reinforced plastics for bridge applications is reduced installation,

handling, repair, and life-cycle costs as well as improved corrosion and durability (Mazumdar).

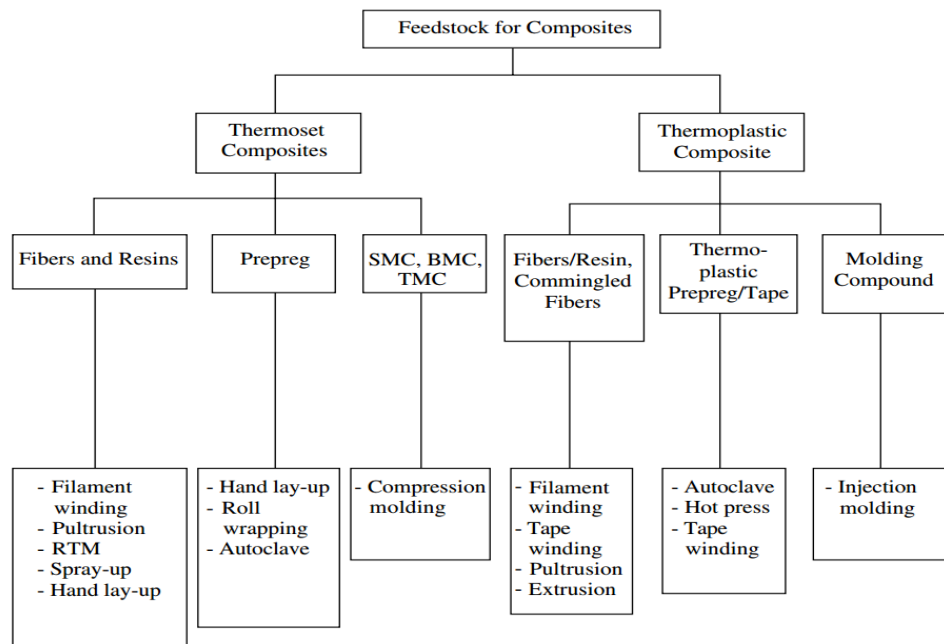


Figure 4.1. Classification of Raw Material (Mazumdar).

4.1 Materials

Fibers:

In a continuous fiber reinforced composite, the fibers provide virtually all the load-carrying characteristics of the composite, the most important of which are strength and stiffness. (These fibers may also be referred to as filaments. In this case, a group of filaments is known as a fiber or fiber bundle.) The multiple fibers in a composite make it a very redundant material, in case the failure of even several fibers results in the redistribution of the load onto other fibers (Reinhart et al.).

Fabric:

The majority of membrane structures have been built using woven fabrics made from a glass-fiber base. These materials are produced on industrial looms that Output rolls

of fabric panels in limited widths. The structural base fabric is usually coated as a measure of protection against UV rays, moisture penetration, and dirt accumulation. (Bechthold) Woven fabrics are used in trailers, containers, barge covers, and water tower blades, and in other marine wet lay-up applications. In a plain, Twill, Satin and other weave patterns, yarns are interlaced in 0° , and 90° directions are equally distributed (Mazumdar).

The essential mechanical properties are obviously tensile strength and stiffness, but also include tear resistance and maximum elongation at break. Fabrics based on glass, polyester threads have tensile strengths in order of 1-10kN/5 cm. The amount of prestressing varies greatly depending on the span, curvature, loading conditions, and other factors (Bechthold).

Woven fabric composites offer interesting advantages with respect to composites laminated from unidirectional plies. The interlacing of the yarns improves the through-thickness behavior resulting in increased impact resistance, for instance. Fabric composites are easy to handle and remain coherent at elevated temperatures, a benefit that allows for the draping of parts with complex geometry (Wijskamp).

Glass Fiber:

The glass is an amorphous material obtained from the molten (melt) state by cooling the liquid at a rate such that no ordered regions (known as crystals) are formed.

Chemically, glass is primarily composed of a silica network. However, pure silica or quartz requires very high temperatures before it can be melted and drawn into fibers.

Therefore, other chemical components are added to decrease the glass viscosity to levels suitable for melting, homogenizing, removal of gaseous inclusions, and fiberizing. The physical properties of the resultant glass are altered to varying degrees

by the type and number of modifiers (Reinhart et al.).

Table 2.1. Glass fiber Composition (Reinhart et al.)

Glass Type	Material, weight %							
	Silica	Alumina	Calcium oxide	Magnesia	Boron oxide	Soda	Calcium fluoride	Total minor oxides
E-glass	54	14	20.5	0.5	8	1	1	1
A-glass	72	1	8	4	...	14	...	1
ECR-glass	61	11	22	3	...	0.6	...	2.4
S-glass	64	25	...	10	...	0.3	...	0.7

Although some glass compositions have been deployed, only a few are used commercially to create continuous glass fibers. The four main glasses used are high alkali (A-glass), electrical grade (E-glass), a modified E-glass that is chemically resistant (ECR-glass), and high strength (S-glass). High-alkali glass, primarily consisting of soda lime silica, is used in applications such as windows and containers. The fiber form of this composition is used in applications requiring good reinforcing properties coupled with better chemical resistance (Reinhart et al.).

Table 3. Inherent properties of glass fibers (Reinhart et al.)

	Specific gravity	Tensile strength		Tensile modulus		Coefficient of thermal expansion $10^{-6}/K$	Dielectric constant(a)	Liquidous temperature	
		MPa	ksi	GPa	10^6 psi			°C	°F
E-glass	2.58	3450	500	72.5	10.5	5.0	6.3	1065	1950
A-glass	2.50	3040	440	69.0	10.0	8.6	6.9	996	1825
ECR-glass	2.62	3625	525	72.5	10.5	5.0	6.5	1204	2200
S-glass	2.48	4590	665	86.0	12.5	5.6	5.1	1454	2650

(a)At 20 °C (72 °F) and 1 MHz.

Initial scientific and engineering understanding of fiber-reinforced organic matrix composites was based on studies of glass fiber reinforced composites. Both continuous and discontinuous glass fiber reinforced composites have found extensive application, ranging from nonstructural, low-performance uses such as panels in aircraft and appliances to such high-performance applications as rocket motor cases and pressure vessels. The reasons for the widespread usage of glass fibers in composites both in the past and in the present, include competitive price, availability, good handling, ease of processing, high strength, and other acceptable properties. Furthermore, the advent of highly efficient silane coupling agents, which are very compatible with either polyester or epoxy matrices, provided a strong and much-needed boost in property translation and environmental durability (Reinhart et al.).

4.2 Matrices

As already mentioned the purpose of the composite matrix is to bind the fibers together by its cohesive and adhesive characteristics, to transfer the load to and between the fibers. The matrix resin keeps the reinforcing fibers in the proper orientation and position so that they can carry the intended loads, distributes the loads evenly among the fibers, provides resistance to crack propagation and damage, and provides all of the interlaminar shear strength of the composite. Furthermore, the matrix determines the overall service temperature limitations of the composite and control its environmental resistance (Reinhart et al.).

4.2.1 Epoxy Resin

Epoxy resins are presently used far more than all other matrices in advanced composite materials for structural applications. Epoxy resins have good physical properties, mechanical capabilities and processing conditions that makes them invaluable by comparison to other matrices. Depending on the chemical structures of the resin and

the curing agent, the availability of the various modifying reactants, and the condition of the cure, it is possible to obtain toughness, chemical, and solvent resistance. The mechanical responses ranging from extreme flexibility to high strength and hardness, resistance to creep and fatigue, excellent adhesion to most fibers, heat resistance and excellent electrical properties. There is low shrinkage during the cure. The chemistry involved in the use and application of epoxy resins is the key to their outstanding performance. All epoxy resins contain the epoxide, oxirane, or ethoxylene group; where R represents the point of attachment to the resin molecule. The epoxide function is usually a 1, 2- or a-epoxide that appears in the form called the glycidyl group, which is attached to the remainder of the molecule by an oxygen, nitrogen, or carboxyl linkage, hence the terms glycidyl ether, glycidyl amine or glycidyl ester (Reinhart et al.).

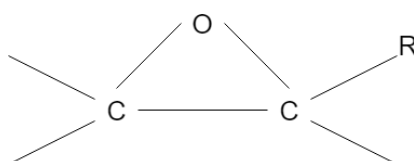


Figure 4.2. Chemical Structure of ethoxylene group (Compiled in draw.io)

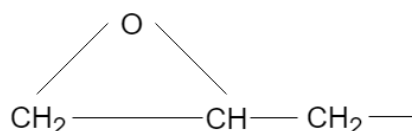


Figure 4.3 Chemical Structure of glycidyl group (Compiled in draw.io)

Curing of the resin results from the reaction of the oxirane group with compounds that contain reactive hydrogen atoms:

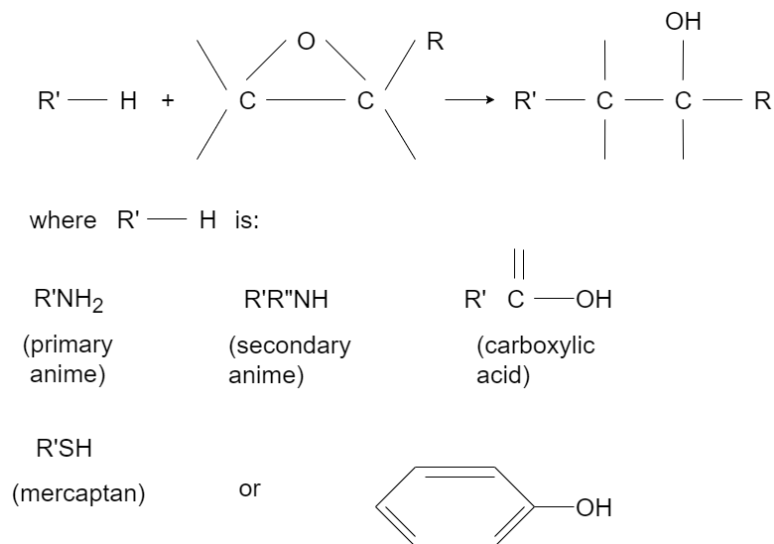


Figure 4.4. Chemical Reaction (Reinhart et al.).

Two other chemical reactions must be considered in the curing of the epoxy resins, the reaction with carboxylic acid anhydrides, and catalysis by acid and base. The carboxylic acid anhydrides, similar to the carboxylic acids, yield ester cross-links. Acid and base catalysis results in the homopolymerization of the epoxide to a polyether; where n can be any number of ether units, depending on the catalyst and the reaction conditions (Reinhart et al.).

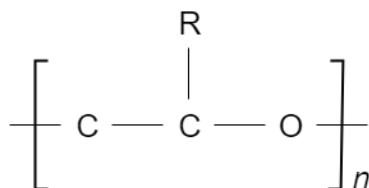


Figure 4.5. Homopolymerization of epoxide (Compiled in draw.io)

The elongation to failure of most cured epoxies is relatively low, for many applications epoxies provide an almost unbeatable combination of handling

characteristics, processing flexibility, composite mechanical properties, and acceptable cost (Reinhart et al.).

4.2.2 Cure Agent

The curing agent selection plays the significant role having the properties like pot life, dry time and wetting. Curing agents can be classified based upon amines or amides groups in the chemical structure (Oman).

- A. Aliphatic (carbon atoms forming open chains) and cycloaliphatic (ring structured aliphatics) amines and polyamines. Amines are ammonia with one or more hydrogen atoms replaced by organic groups;
- B. Amides and polyamides. Amides are ammonia with a hydrogen atom replaced by a carbon/oxygen and organic group.

Amine-based curing agents are considered to more durable and chemical resistant than amide based curing agents and Amides, are more surface tolerant and less troubled by moisture (Oman). Amines with non-benzene ring make the curing agent best suitable for the water resistant applications. These particular polyamines form the basis for today's cutting-edge underwater epoxies.

- C. Cycloaliphatic curing agents. The cycloaliphatic curing agents provide better water/moisture resistance, weather ability, low blush and water spotting, and better chemical resistance (Oman).

5. LITERATURE ON RECONFIGURABLE MOLD TECHNIQUES

5.1 Introduction

Research into facade panels has been predominantly focused on two main areas: manufacturing processes for constructing unique composite panels and materials used to create panels. Using flat and thin sheets of specific materials such as plastic or metal and making them into a bendable shape requires not just the knowledge of material properties but also knowledge of manufacturing possibilities. Solid dies, static molds are frequently used to achieve the desired shape of the panels. In the manufacturing process, materials are pressed into a die of a specific shape and fabrication on the molds to achieve different shapes. With every new shape of the material, a new die and mold are necessary. Every individual mold makes the manufacturing process a bit of a challenge as it becomes mostly suitable for larger products. When it comes to smaller products that need to be frequently reproduced, replacing mold with each shape would be quite expensive. A new manufacturing solution is strongly desirable, to cut the expense of mold making, which is the primary concern of many industries.

In case of smaller materials, reconfigurable molds would be one of the desired solutions. This manufacturing problem is not something that only affects building industry. It is also present in other industries such as automotive, marine, aerospace, transportation and energy industry. All these industries have faced with the costing issue where specific shapes have to be manufactured in a high variety and with impeccable accuracy. Therefore, a need for researching facade panels' materials and manufacturing processes is still current and vital topic across not just the architectural, but many other industries as well.

5.2 Conventional semi-automatic mold techniques:

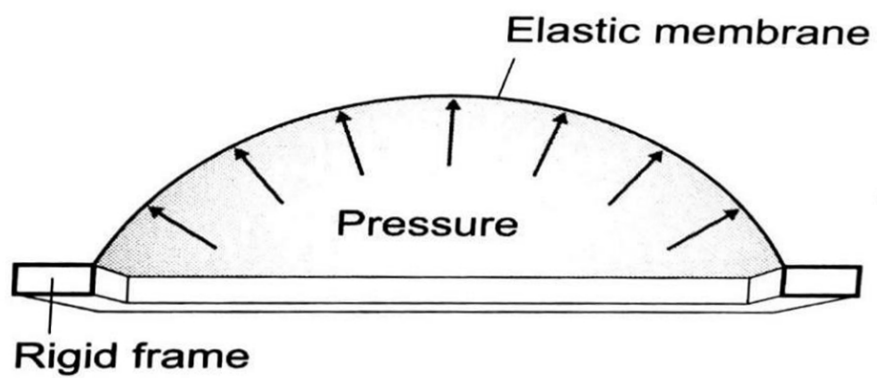


Figure 5.1. Pneumatic form-finding method (Bechthold).

In Roel Schipper's article, Renzo Piano (1969) was the first who carry out comprehensive research and development on the flexible mold technique about the

manufacturing of architectural elements. He developed a process of flexible mold method to produce double-curved fiber-reinforced plastic elements. These elements were manufactured and constructed in free form 3D structures using plastic by Piano (Schipper).

Later studied by Oosterhoff 1969, stated that the mold could also be used for the construction of reinforced concrete shells. Piano's prototype of flexible mold consisted of a grid of plungers and a flexible surface on top. The plungers would shape 3D curved elements of plastic structures, that would together be assembled into free-form pavilions. Piano constructed a number of experimental pavilions, for example, the one shown in Figure 5.3. This innovative machine, named "stampo deformable" or "deformable mold," is shown in Figure 5.2. This machine could read from a scaled model of a free-form building the building height at a grid of x-y-coordinates, and translate this to full-scale panels manufactured in plastic structures, a sort of 3D-printing method (Schipper).

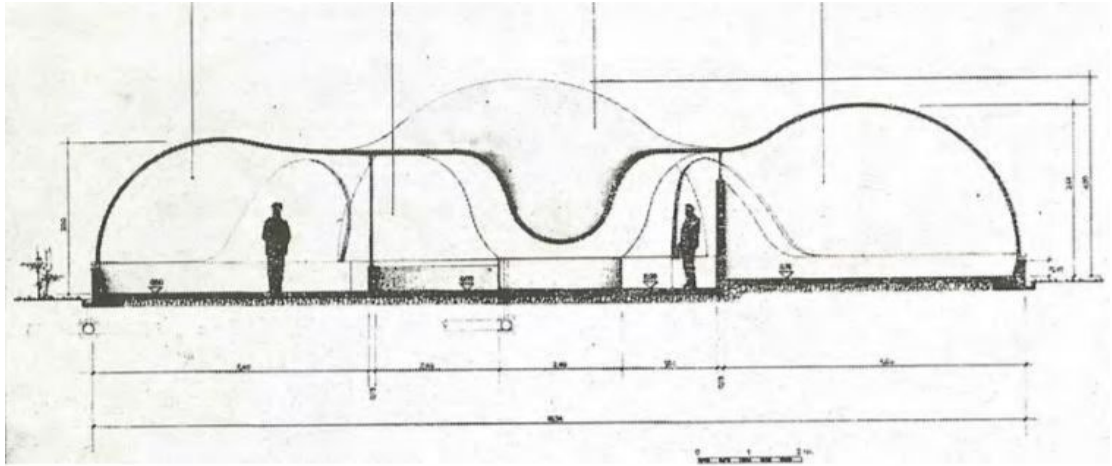


Figure 5.2. Morphological study of a pavilion in glass-fiber reinforced plastic, source: Piano [1969] (Schipper).

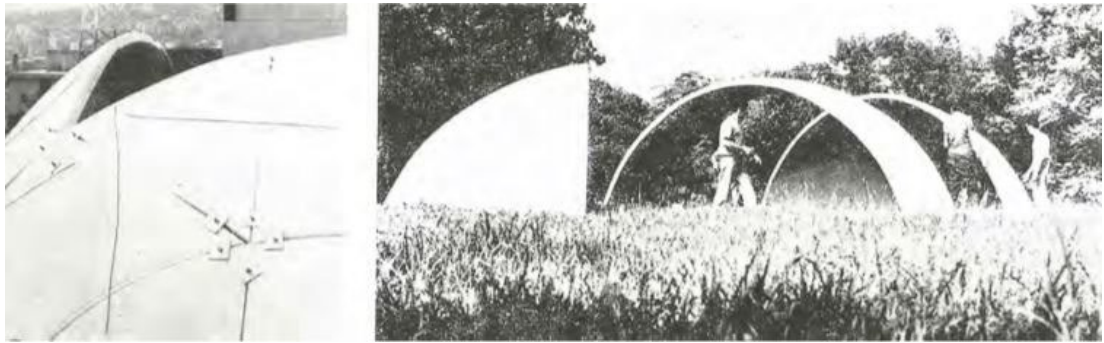
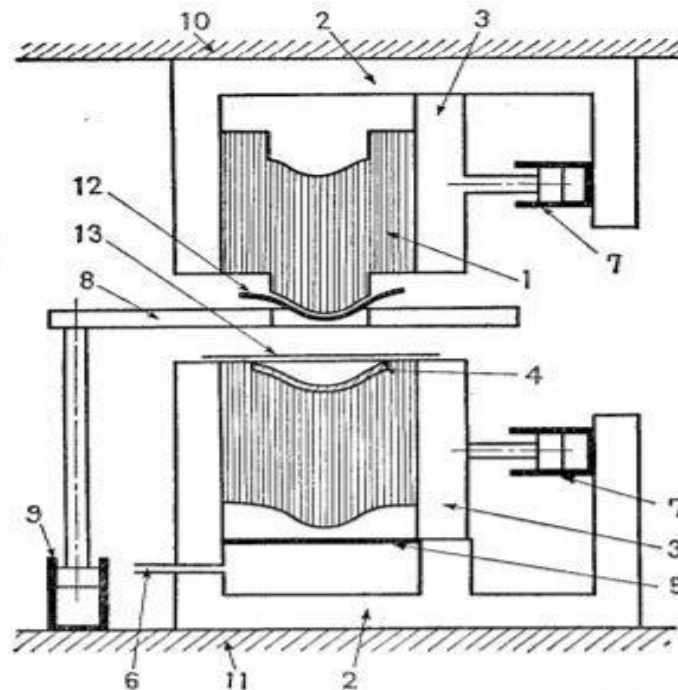


Figure 5.3. Pavilion made out of triangular double-curved plastic panels, source: Piano [1969] (Schipper).

researchers followed the similar principles of configuring large numbers of pins with a small diameter and bounding them tightly together (Nakajima).



1. Wires, 2. Retainer (main part), 3. Slide plate of the retainer, 4. Sheet model, 5. Rubber sheet, 6. Compressed air intel, 7. cylinder for locking, 8. Blank holder, 9. Cylinder for locking, 20. Upper table of a press, 11. Lower table of a press, 12. Rubber sheet for protecting sheet metal, 13. Blank (sheet metal) (Nakajima)

Figure 5.5. Structure of the experimental device for a press working (Nakajima).

In late 1990's, Kleespies and Crawford described a principle that was built on the similar idea originated by the famous architect Renzo Piano. In the same manner as Piano, the researchers used the pins with the significant distance between them. They further placed a rubber membrane in between the pins with the intention to create a styrene thermoplastic. Differently, from Piano, Kleespies and Crawford chose to use a vacuum pressure in their research to maintain contact between the rubber membrane and the pins (As shown in Figure 5.6.). Also, Kleespies and Crawford investigated a relationship between the thickness and Young's modulus in inserted rubber material membrane. The conclusion they were led to in the aftermath of their research was that

there are limitations in the surface geometry of the new-formed parts. In addition, in looking to create a free-form shape, one has to restrict the radius to a certain minimum so that a feasible, flexible mold system could be designed. Kleespies and Crawford describe the basic relationships between mold design of the surface quality and the minimum radius of curvature. The prototype was made by vacuum fusing of polystyrene thermoplastics and, Acrylonitrile Butadiene Styrene. The variable configuration of the mold makes the process quick and, automated. By automation, predetermined shapes can be achieved more efficiently with the help of computer surface models. The freeform geometry of the curved surfaces is achieved by variable vacuum forming mold prototyping, but with limitations of accurate curvatures radii and smoothness of the curved surface (Kleespies and Crawford).

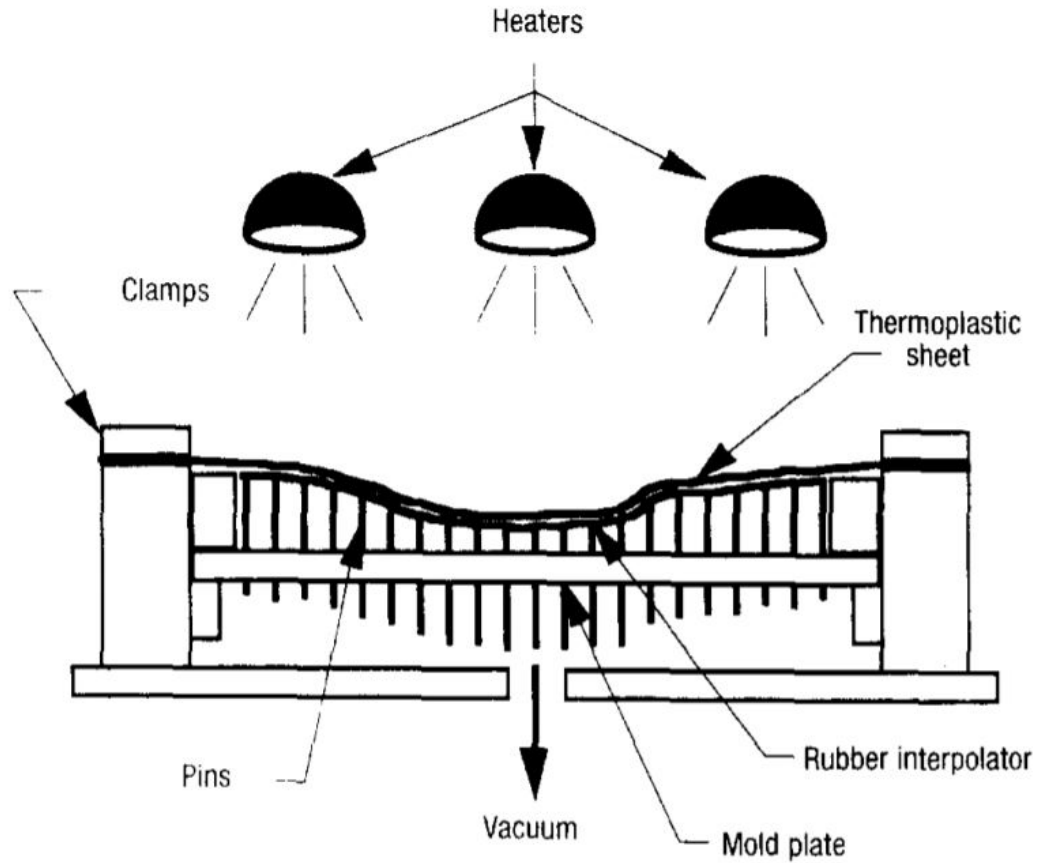


Figure 5.6. Variable Configuration Mold Thermoforming (Kleespies and Crawford).

Pinson's patent on forming sheet metal apparatus has two sets of an equally spaced pin actuator matrix. The first set of movable pins are arranged in a matrix array on the support members. The second set of movable pins disposed on the other of said support members in positions corresponding to the rams of the first set, each ram of one set being substantially in alignment with a ram of the other which act as the punch and die. The pin actuators are threaded and are freely movable, with an attached motor. The second set of pins matrix are aligned to the first pin matrix. The extremities of the pins decide the curve of the metal sheet surface when pressure is applied to the pin matrix from both ends to get workpiece in the desired shape (Pinson).

Soderberg et al. describe the invention of an actuator based flexible tooling system. The whole assembly has cylindrical actuators, the actuators managed by vacuum and air supply line with the help of network interface so that each position may be addressed separately and gives the desired shape on the surface of the mold. The movable actuator has corresponding connectors for receiving the vacuum and air supply as well as for interfacing with the bus. The Individual position has a unique address so that an actuator may be placed at a location. All the longitudinal position is adjusted individually by using a computer. The actuators are addressed on the bus to command the actuator to raise, lower, lock in position and, supply vacuum to the desired structure can be reflected the contour of the work panel (Soderberg).

5.3 Contemporary Molding Techniques

In the mid-2000s, mechanical engineer Boers developed a “flexi-mold system,” another way of creating reconfigurable mold (As shown in Figure 5.7). One of the main points of his research was the use of a matrix of pins that could be reconfigured in short amount of time and the variety of shapes. This would allow fast prototyping experiments and a small collection of uniquely shaped metal sheets. Furthermore, the method could be applied to other materials such as thermoplastics and not just a metal. The other areas of Boers’ research covered the elasticity of the deformed material (the rubber sheets) used as interpolators. He ultimately wanted to create a smooth surface without the visibility of the pins. Also, when it comes to reconfigurable molds, Boers saw the application of his research in a field of architecture and construction materials (Boers).

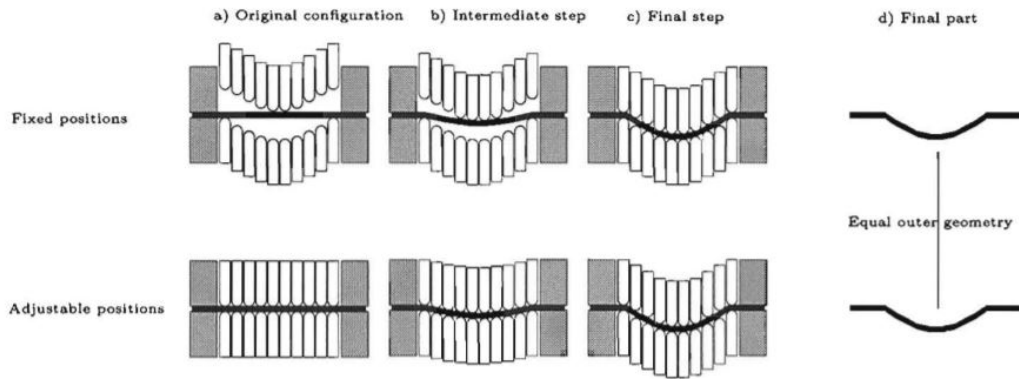


Figure 5.7. Optimum forming and multi-point deformation (Boers).

According to Groeneveld, the manipulation of the flat metal sheet can also be achieved using a single-sided die and the explosion. The metal is placed on the die that was previously milled in a required shape. The explosion is detonated to press the metal into the die, which happens within few milliseconds. The benefit of this process is considerable freedom in creating a shape that will allow large plates (up to $10 \text{ m} \times 2 \text{ m}$) and various thicknesses (0.3 mm – 60 mm). It is also suitable for many different metals. This method, however, is not the best fit for concrete, since the explosion forming principle relies on the plasticity of metals. Plasticity of metals is a material property typically not present in concrete, at least not in the same quantity (Groeneveld).

Rao and Dhande are of the opinion that flexible surface tooling is based on the concept of the discrete approximation to a continuous surface of a mold or a die. It consists of some closely spaced multiple rigid surface tool elements, known as indentors, each of which is a surface element of an expected contour. The height of the indentors can be adjusted to approximate the desired surface shapes. The positioning of each indenter can be carried out either manually or through the computer. By placing a deformable elastomeric sheet over the indentors reduce the

tool surface unevenness (shown below in Figure 5.8). The flexible sheet draped over the discrete surface provides a continuous surface required for the tooling application. The intendorors are adjustable and can create a variety of surface shapes by adequately adjusting the heights of surface tool elements. Experiments with new shapes and incorporating design changes will be much easier once such tooling is made available. Computational simulation of the proposed tooling is carried out for feasibility studies. Computational simulation involves the deformation analysis of rubber-like membranes in multiple contacts by FEM. The sheet-forming processes and composite layup get easy on this tool (Dhande and Rao).

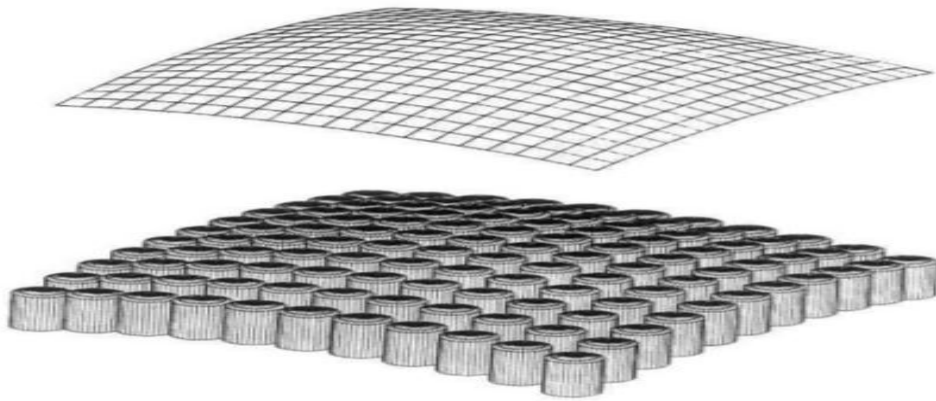


Figure 5.8. A discrete approximation to a continuous surface (Dhande and Rao).

In 2010 Rietbergen and Vollers invented a method of flexible mold, which was a cost-effective solution for manufacturing of panels but also required less labor. In their research, they described the formation of a double-curved panel by using the flat panel which consists plastically deformable flat surface (As shown in Figure 5.9). The primary support construction enables mold to get a predetermined shape. The double curve is obtained by alignment of primary and secondary support construction. Unlike the primary construction, the secondary supporting construction is adjustable. The

whole assembly is formed like a mat comprised of numerous flexible sticks arranged next to each other. These sticks are kept at a certain distance from each other to provide a surface to the double-curved panel to fabricate (Rietbergen and Vollers).

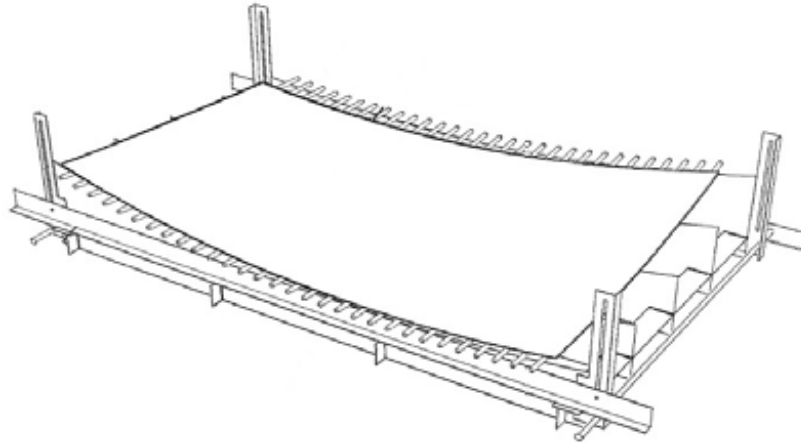


Figure 5.9. Flex-Rod' (Rietbergen and Vollers).

Rooy et al. give the different molding techniques that have been used to make 3D surfaces with prefabricated elements. The prototype contains a tensioned flexible layer, and the flexible layer is manipulated with the use of manually set actuators, an amount of tension and an inflatable arrangement. The actuators are only positioned at the edges and consist of upper and lower array arrangement as shown below in Figure 5.10. The accuracy of the edges is essential for the edge transitions of the panels. The size of the mold is 1200 mm × 1800 mm. This flexible mold can produce polyester and composite panels that have been made for a three-dimensional curved facade with the help of the vacuum injection molding method (Rooy et al.).

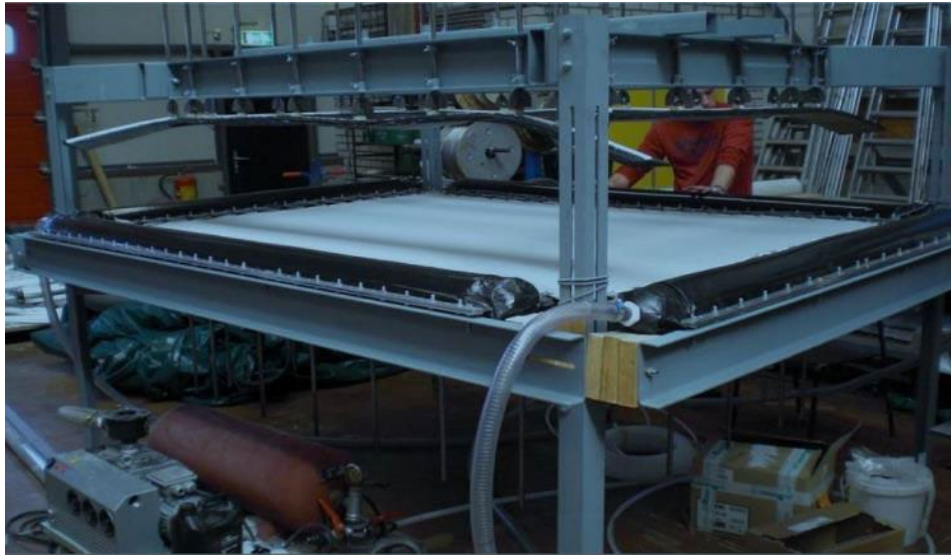


Figure 5.10. The mold attached to Injection molding method (Rooy et al.).

In a paper published on Mass Customization of Double-Curved Metal Facade Panels using a new hybrid sheet metal processing technique by Ghang Lee and Seonwoo Kim develop a new hybrid sheet metal processing technique to fabricate double curved metal panels for the Dongdaemun Design Park are reported. “DDP, designed by Zaha Hadid, has an unusually high percentage of double-curved panels. Among the 45,000 facade panels, approximately 22,000 panels are double curved” (Lee and Kim). The structures were very complex as there are a large number of different panels used were different shapes. As a result, the researchers proposed three alternative methods for fabrication of the panels.

The first alternative discussed was a multipoint forming machine with a rubber pad between the sheet metal blank and computer-controlled posts. The problem associated with this was about the quality of finish because the metal blank can be wrinkled when pressed. The second alternative considered was hydroforming and multipoint forming. In this method, there should be multiple posts on one side of the metal sheets instead of multiple posts on two sides of the metal blank. The hydraulic pressure used

was too strong for the multiple posts as it left dents on the panels. The third approach considered was the use of multipoint stretch forming shown in Figure 5.11., curved shapes can be formed by stretching and pressing the fixed sheet metal blank with computer-controlled multiple posts. This test was the most viable solution for fabricating the Facade panels in the present era (Lee and Kim).

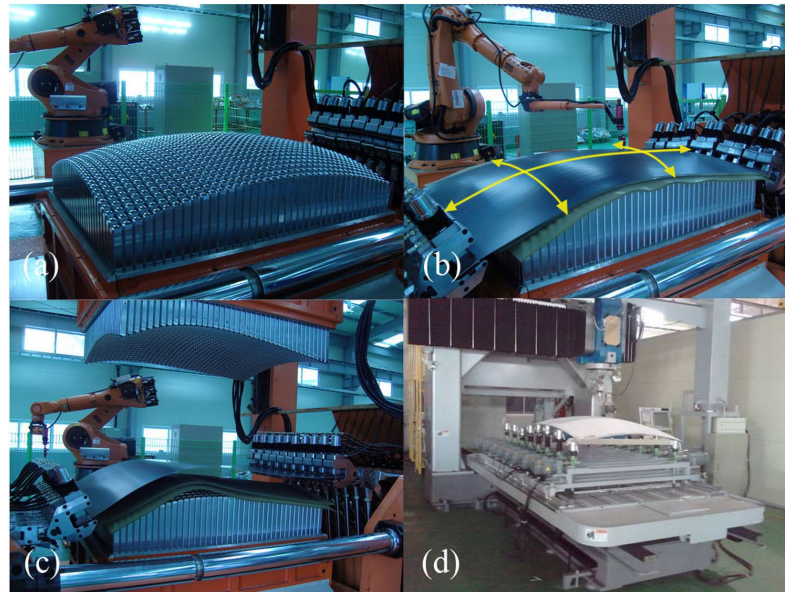


Figure 5.11. Multipoint stretch forming machine: (a) medium-scale computerized multipoint stretch forming machine; (b) mildly curved panels are fabricated using two-way stretch forming only; (c) complex shapes are pressed once more with the upper multipoint forming mold; (d) the curved panels are cut and perforated with a special computerized laser-cutting machine (Lee and Kim).

In their invention, Kristensen and Raun provided a method in which double-curved molding surface is reconfigurable in a molding tool by using flexible top surface. The flexible surface has flat rhomboid elements having elasticity in top surface material aligned in the movable form in two or more rotating layers. The top membrane of the flexible material is attached to the bottom membrane of an elastic deformable layer. The assembly of different layers is assembled and attached to the top of the actuator matrix having variable height limits. The surface of the flexible layer is achieved by

the corresponding position of the attached actuator matrix. The top layer assembly is capable of forming a double-curved and smooth surface. Assembly of the different layers including the rhombuses structure can be bent expediently, due to its flexibility. After the top structure achieves the desired shape, the flexible assembly returns to its original shape without any change in properties and shape (Raun).

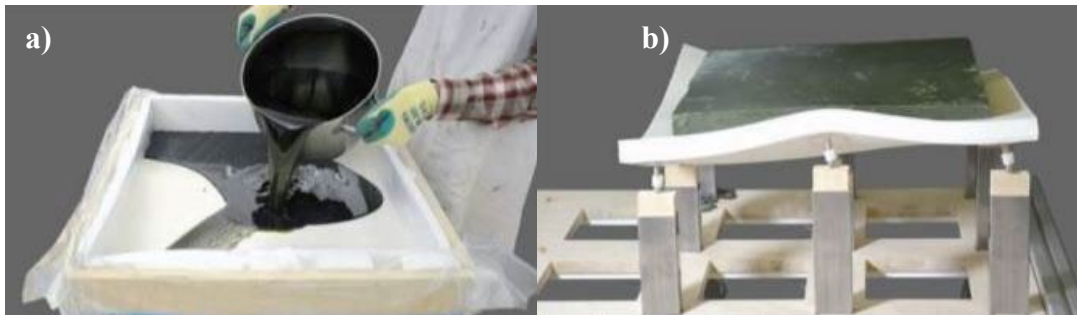


Figure 5.12. a) In left Casting hot wax in mold and b) right Formed wax element on the mold (Oesterle).

Wax is used as a mold material for “Zero Water Free-Formwork.” A flexible layer resting on controller actuator is used to define the shape. A digital geometry model is used to retrieve the settings for the actuators. The flexible layer used in this process is a closed-cell plastic foam. A two-mm silicone layer is applied above this flexible layer. The silicone layer facilitates the easy removal of the wax and prevents traces. After the wax formwork is produced through the flexible actuated mold technique, the reinforcement material is placed on the formwork and left it to sit for some time to get cured. Once the concrete is cured, the formwork wax can be removed. The wax elements used in this process, after melting and filtering, can be recycled to produce new molds as shown in Figure 5.13 (Oesterle).

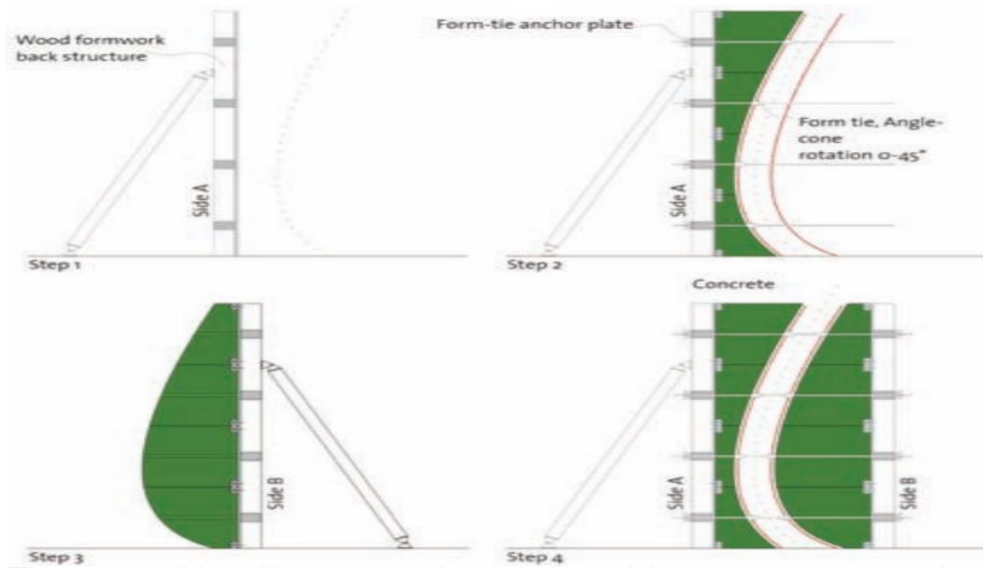


Figure 5.13. Handling procedures for 2-sided formwork on-site: 1. placement of the support structure side a; 2. attaching of wax elements, tie rods and form ties; 3. assembly of side b; 4. attaching side a and b. (Oesterle)

5.4 Conclusion

Table 4. Different mold techniques

Mold Technique	Structures	Method	Authors
1. Pneumatic form-finding method	Synclastic shape (pillow-like form), Concrete shell structure	Semi-Automatic	Heinz Isler (1954)
2. Stretch forming mold technique	Double-curved Shape: Metal sheet	Semi-Automatic	Nakajima (1960)
3. Flexible mold Technique	Double Curved shape: Reinforced plastic structure	Semi-Automatic	Renzo Piano (1969)
4. Stampo Deformable mold technique	Double Curved shape: Reinforced concrete shells	Semi-Automatic	Oosterhoff (1969)
5. Stretch forming	Double curved	Semi-	Pinson(1980)

apparatus	surface: Metal Sheets	Automatic	
6. Variable Configuration mold thermoforming mold	Curved surface: Polystyrene and Acrylonitrile Butadiene Styrene sheets	Semi-Automatic	Kleespies and Crawford (1990)
7. Actuator based flexible tooling system using vacuum	Double Curved shape: Reinforced concrete shells	Semi-Automatic	Soderberg et al(1998)
8. Flexi-mold multi-point deformation system	Unique shape, Metal sheets	Automatic	Boers (2000)
9. Flexible surface mold	Double Curved: Sheet structures	Automatic with Computational simulation	Rao and Dhande (2002)
10. Single-sided die and the explosion method	Curved surfaces: Metal sheet panels	Semi-Automatic	Groeneveld (2008)
11. Flexible Mold	Three-dimensional curved façade: Polyester composite panels	Semi-Automatic	Rooy et al (2009)
12. Plastically deformable mold	Double-curved panel: Reinforced concrete panels	Semi-Automatic	Rietbergen and Vollers (2010)
13. Reusable wax Free-Formwork method	Double-curved: Concrete Panels	Semi-Automatic	Oesterle, S et al(2012)
14. Multipoint stretch forming Method	Three-dimensional curved façade: Metal Panels	Automatic computer controlled	Ghang Lee and Seonwoo Kim (2013)
15. Double-curved	Double-curved:	Semi-	Kristensen and

molding surface Method	Rhombuses Concrete Panels	Automatic	Raun (2015)
---------------------------	------------------------------	-----------	-------------

After careful review of previous works in the automation of different molding processes, we noticed many disadvantages in the way the molding processes are carried out. Making use of the drawbacks of these conventional techniques, developed the automated molding technique, which is economical, less labor intensive, and efficient in scenarios which involve unique and complex structures. In this molding technique DC motor-driven actuator matrix has used, to achieve the desired curvature on the flexible membrane with the help of computer controlled Three-dimensional surface software which makes this method unique and more efficient than other invented mold making methods. Automation is relatively more economical for production cycles and less time consuming than the conventional methods with help of textile composite in the architectural facade industry.

6. EXPERIMENTATION AND PROTOTYPING

Experiments are conducted in all engineering fields which aid in decision-making process and discovery of novel phenomena that can lead to new products or technologies including new product development, new process development, and improvement of existing products or processes (Montgomery).

Most processes can be described regarding several controllable variables. By using designed experiments, engineers can determine which subset of the process variables has the most significant influence on process performance (Montgomery).

The results of such an experiment can lead to

1. Improved process yield
2. Reduced variability in the process and closer conformance to nominal or target requirements
3. Reduced design and development time
4. Reduced cost of operation

Experimental design methods are also valuable in engineering design activities.

During these activities, new products are developed, and existing ones are improved (Montgomery).

In the beginning, the experiments were performed by keeping all factors constant while varying the geometry of the flexible membrane of the prototype. Later, we found that the structures were affected by other factors like the strength of the actuators, thickness of the flexible membrane, the density of the actuators heads, and then some trials were performed to see the effect of each factor on the different shaped structures. It was also observed that every factor was changing the geometry of the panel and in future work, these can be improved.

During the experiments, following parameters affected the structural geometry of the panels:

1. Non-measurable parameters:
 - Geometry of the prototype structure
 - Height of actuators
 - Thickness of the Flexible membrane
 - Density of actuators
 - DC motor driven actuator's strength
 - Vacuum bagging compression force on actuators
 - Fabric stiffness
2. Measurable parameter:
 - Height of structure at individual actuator

This research work was done in two different segments:

1. Stage first was to develop an automated flexible mold prototype.
2. Stage second was to perform experiments to form fiber glass textile composite panels to prove the prototype concept.
 - a. Samples are repeatable
 - b. Samples are same as ideal 3-D design.

6.1 Preliminary Phases of the mold Prototype Development

6.1.1 Static Mold

Steps involved in static mold making process:

1. The wooden board of 60.96×60.96 sq. cm. was chosen for the mold making process.
2. The double curved geometry was designed using Rhino 3D CAD software.
3. Then the board was milled into the double curved shape using the CNC milling machine.
4. Then various composite panels were formed on this wooden board mold by hand layup process by using fiberglass and matrix keeping 3:1 ratio of the fiber to the resin matrix.

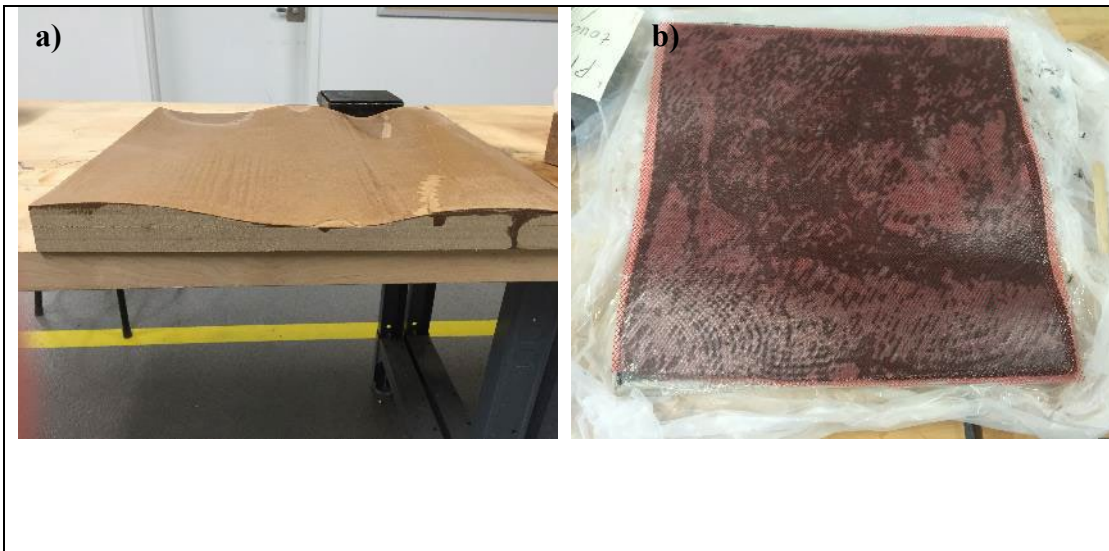


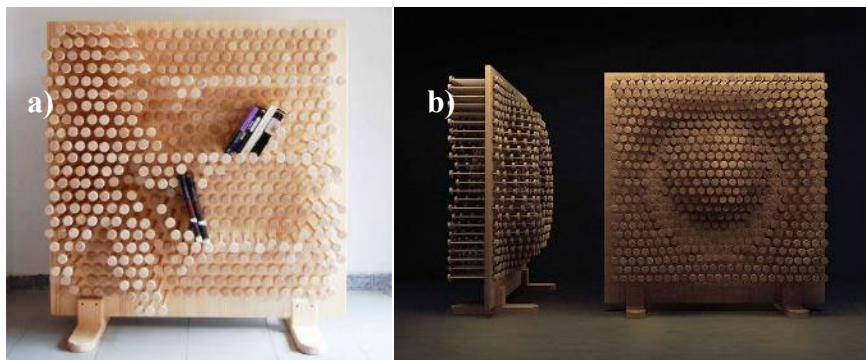


Figure 6.1 Curved Panel formation on Static Mold a) Wooden board CNC milled mold b) Hand lay-up of composite materials and matrix c) Final free form double curved panel d) Final free form double curved surface (Pictures courtesy Gurjar)

Static molds have been in use for a long time. This process has generated most of the older free-form structures. However, this mold making process is labor-intensive, time-consuming and restricted to a single shape. As this is an inefficient process, it allows the scope for improvement.

The suggested improvements are as follows:

1. Automatization of mold can mitigate the labor-intensive process of the static mold making. We got this idea of pin bed game where the pins are arranged in series of equidistant rows and columns. When the force is applied to the top of the pin bed, it gives the similar shape of the object on the surface.
2. We need a mold which is easy to reuse by changing the top surface of the mold in



desired curved panel structure.

Figure 6.2 a) Pin bed shelf and b) game (Rogers).

The next challenge was to create a mold which would be reusable so that we can reduce the cost of mold making process for the formation of the new curved panel.

6.1.2 Movable surface mold using pin bed concept

After working on static mold, the next step was to find a way to manipulate the surface of the mold. To create the top surface of the mold, the concept of pin bed game was used. The model structure of size 30.48×30.48 sq. cm using 16 wooden pins was made with the help of CNC milled polystyrene dome shape structure in the bottom was placed below the 4×4 grid of pins. This caused the pins to be elevated along the contours of the polystyrene dome.

Using hand layup process the composite material and matrix were placed on the top of the elevated actuator pins. This allowed the composite material and matrix to take the shape of a dome of the dimension 30.48×30.48 sq. cm size of the panel as shown in figures 6.3 below.

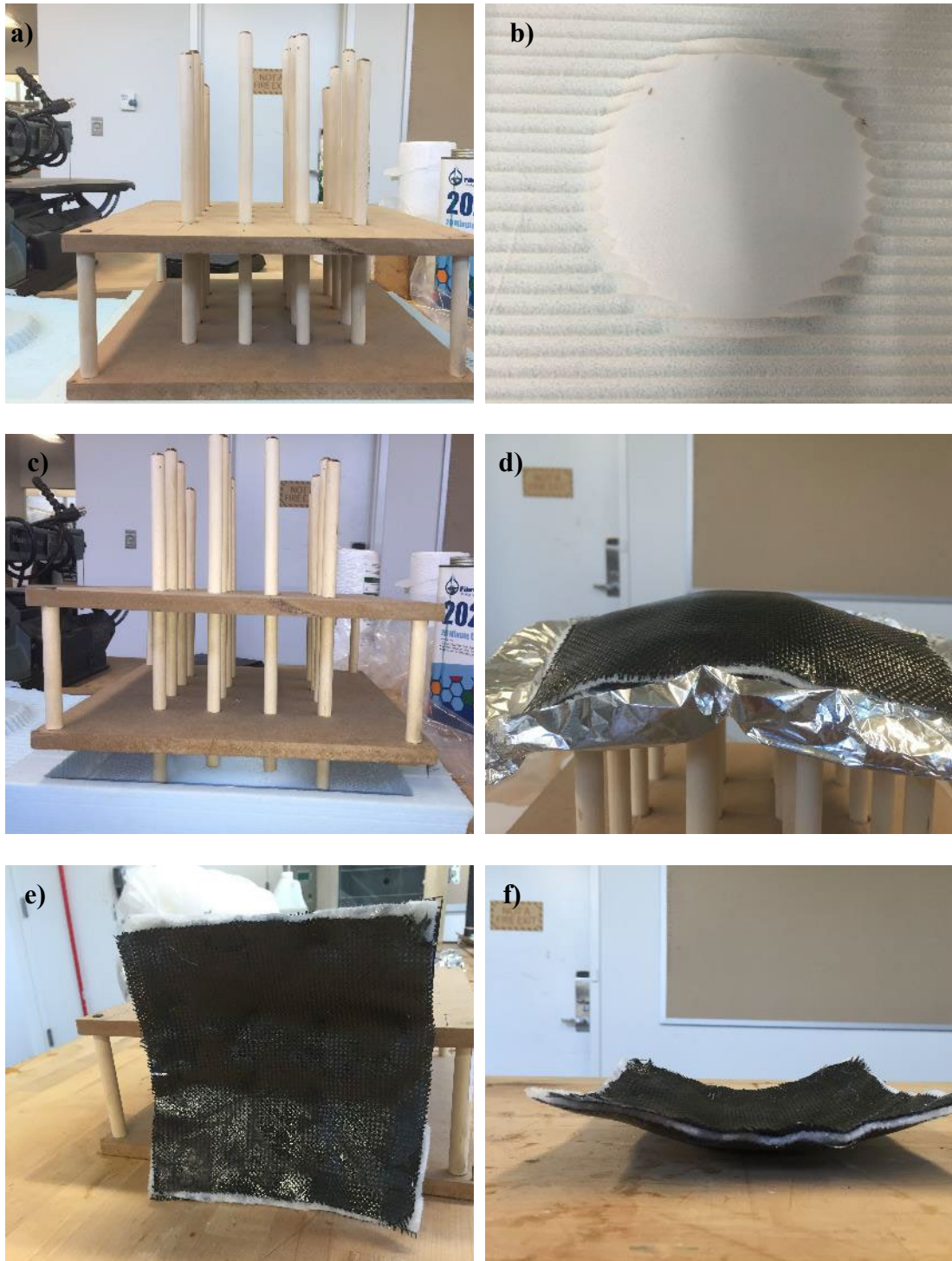


Figure 6.3 Process of curved panel formation by pin bed method a) Pin bed frame, b) CNC molded shape, c) Pin bed with curved structure, d) Composite layup, e) Drying Panel, f) Finished panel (Pictures courtesy Gurjar)

6.2 Stage I: Proposed Prototype Method

After doing numerous experiments on different molds, recognized a need of automated shape changing mold with the help of digital and physical work to create varying size facade panels for free-form architectural structures. The goal of reconfigure mold prototype was to move towards better and efficient way of automation of mold and curb the mold waste and expensive mold making process.

6.2.1 First Step: Digital to Physical Actuation

The design and interface control are achieved through Rhino 3D/Grasshopper Firefly plugins, which translates the composite panel surface geometry into required heights of the actuators, which is limited to 25.4 mm in upward direction, in the form of binary code. This binary code is sent to Arduino microcontroller via the grasshopper firefly plugin, which determines the initial support heights according to the distance between the initial point to the height of the actuators which is attached to the flexible membrane. The Arduino microcontroller interprets these signals for the design and propagates to the relay array. The relay array causes the actuators to move in the vertical oscillating motion defining the curvature of the top flexible silicone surface.

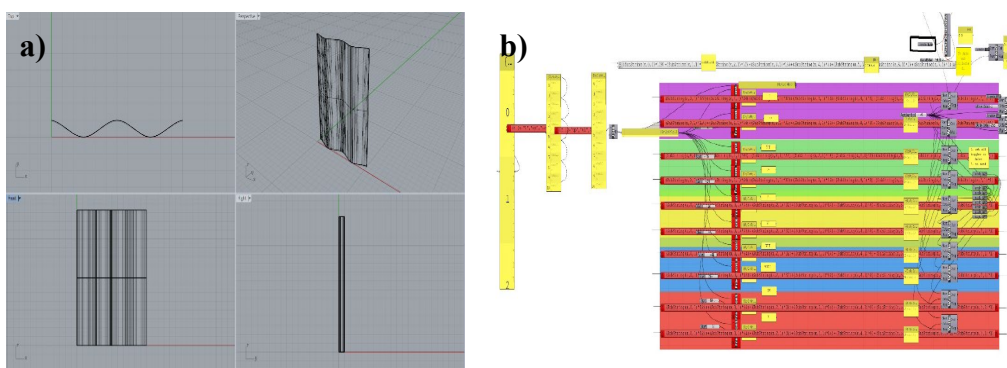


Figure 6.4 Design of panel on a) Rhino and b) Firefly Plugin script for shift register (Ku)

6.2.2 Second Step: Construction of Prototype mold device

The development of the prototype mold by keeping all three major mold techniques and designed a shape changing reconfigurable flexible mold. The development process considered design to manufacturing process. During the design process, cost implications of applying composite panels were assessed through parametric modeling and optimization tools. The scope of work is to identify the custom penalization and analysis of the performance of the materials. The material process involves a hybrid process of automated and manual processes to fabricate the panel structure.

For this research, prototype frame size is 67.945 cm × 53.34 cm and the structural surface of 38.1 cm × 30.48 cm was created with five rows of eight actuators with a total of 40 actuators with a maximum stepping height of 25.4 mm for each actuator. The number of actuators and size of a mold can vary according to the required size of the composite panels. The distance between the actuator heads was 7.62 cm. These actuators are placed in a close spaced matrix which is DC Motor controlled by an Arduino microcontroller with shift registers and relay. After working on few flexible surface materials, found silicon membrane was best suitable for shape changing applications. The matrix of actuator heads was interconnected through rubber silicon sheet of 2 mm thickness which ensures better curve and smooth surface of the panel structure after use of the different thinkness of flexible membrane. This flexible membrane allows the structure to drape and form curved surfaces on the flexible silicon membrane. The actuator is driven by computer 3D rhino software that allows for the mold configuration to change in desired structure. This method ensures reduced tooling costs for the scenario where every structure is unique as the same setup can be used for different panel specifications. On receiving instruction from the

system, vertical actuator heads form a closely spaced geometry. The individual actuator creates the specified curve on the flexible membrane which can easily be transferred to composite panel. The flexible membrane holds the composite material and facilitates vacuum bagging process. It also behaves like a barrier between the composite material and the actuator matrix. The interface control is achieved through Rhino 3D/Grasshopper, Firefly plugins which translates the composite panel surface geometry into required heights of the actuators and reflect on the flexible silicone membrane. This prototype is suitable for lay-up techniques, pre-preg construction, and spray process. The technology promises reduction in the tooling cost provided the production volumes are at a level, and high initial investments are justified. This prototype is highly automated and can create smaller elements that can be manufactured at any place and assembled in an architecture free-form structure.

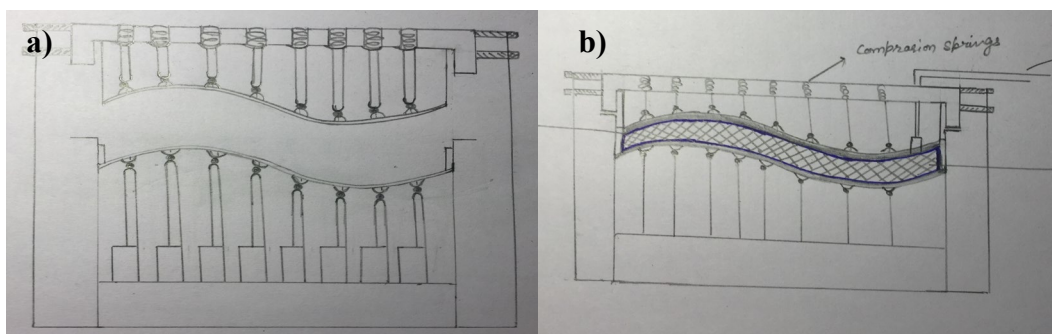


Figure 6.5. Drawing of Prototype Design a) open and b) closed (Drawn by Gurjar).

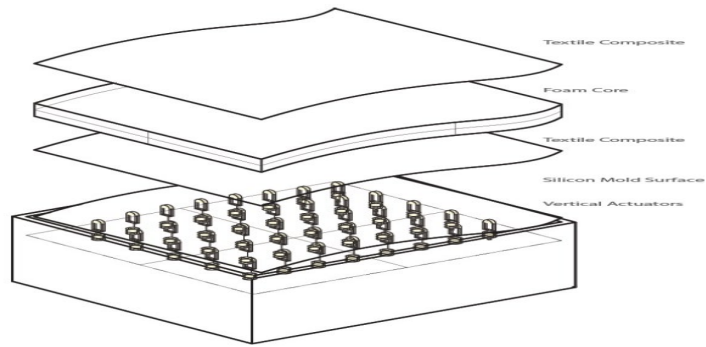


Figure 6.6 Prototype Mold assembly with Silicon flexible membrane attachment with vertical actuators (Ku).

These are the components used for flexible mold prototype:

- a) Flexible Surface: Silicone rubber sheet made of 20T mix of A1: B1 and mold silicone rubber in size of 68.58 cm × 55.88 cm and 2 mm thickness.

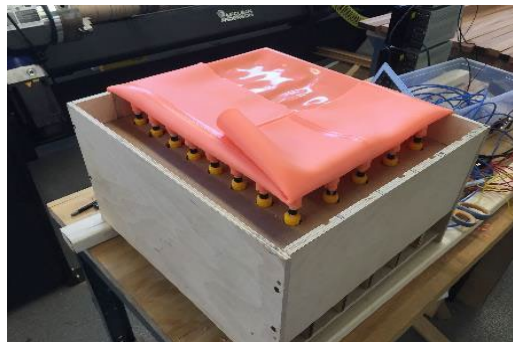


Figure 6.7. Top flexible silicon rubber membrane (Picture courtesy Gurjar)

- b) Arduino: Receives the code and transfer to actuators with the help of relays in binary code.

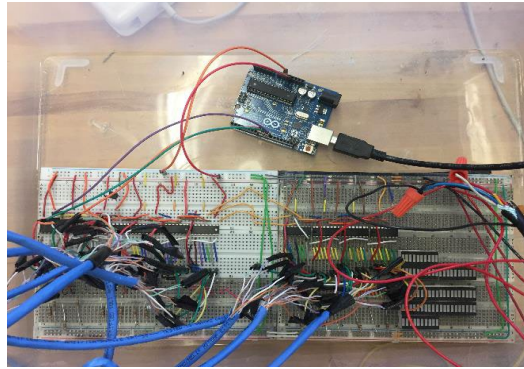


Figure 6.8. Arduino Microcontroller (Picture courtesy Gurjar).

c) An array of Actuators: 40 Nos. D.C. driven Motors.

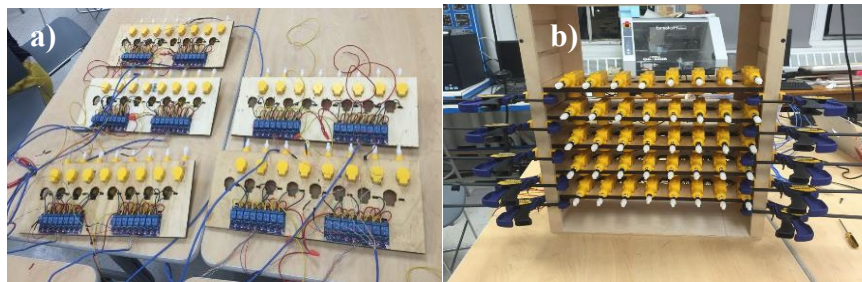


Figure 6.9. Actuator Matrix a) Actuators assembly and b) Actuators inside assembly (Picture courtesy Gurjar).

d) An array of Springs: Assembly of 40 top male compression springs as male mold surface.

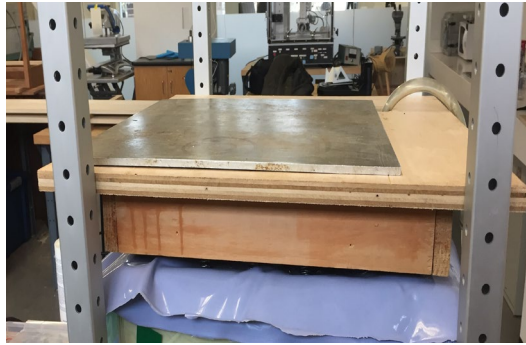


Figure 6.10. Male spring Top (Picture courtesy Gurjar).

e) The framework of Prototype: Wooden and Steel.



Figure 6.11. Prototype Mold (Picture courtesy Gurjar).

6.2.3 Stage II: Production process of composite Architectural Panel

Glass composite panels have maximum design freedom for curved designs for facade elements. Composite made facade panels require significantly less maintenance, lightweight and more resistant to corrosion than the other metal alloy panels.

a) Preparation of Materials

1. Fiberglass fabric: 2 fabric pieces of 90 GSM (2x2 Twill fabric), Company: Fiberglast
2. Resin 2000: Medium viscosity resin, Company: Fiberglast

3. Cure 2060: Pot life of 60 mins, Company: Fiberglast
 4. Wax
 5. Release Fabric from Company: Fiberglast
 6. Perforated Film from Company: Fiberglast
 7. Breather fabric: Nonwoven mesh
 8. Vacuum Bag: Stretchlon 200 bagging film, Company: Fiberglast
 9. Vacuum Pump: Type 322007, Company: IS Leroy Somer
 10. Mastic sealant from Company: Fiberglast
 11. The plumbing system
- b) Lay up of Material: Manually lay up of components.
- c) Vacuum Bagging process:

Manufacturing process of composite panels:

1. Lay down a protective film layer on the flexible membrane of the prototype.
2. Cut two separate 90 gsm twill glass fabric and arranged them in the Zero-degree direction in 38.1 cm × 30.48 cm shape and place them on the flexible silicon rubber membrane.
3. Prepared epoxy resin and cure matrix in 3:1 ratio as per material weight in a container and mix it thoroughly and spread evenly on the fabric.
4. Then placed release film layer on desired structure.
5. Prepared breather layer material and placed on a piece equal in size of the release film.
6. Used mastic tape and adhered on the perimeter of the work surface around the wooden prototype frame for ensuring a closed space without any leakage.

7. Before enclosing the entire space punched a hole in the bagging film just big enough to fit the vacuum adapter.
8. Attach vacuum hose to vacuum adapter and turn the vacuum pump on with 14 psi pressure to remove the air bubble and unevenness of the panel.
9. The pressure created because of vacuum causes reinforce glass fabric and resin matrix to squeeze together.
10. Then placed a spring assembly on the top of the panel structure to provide an equal amount of compression at each point of the actuator head.
11. Vacuum until excess epoxy resin and curing agent matrix is seen bleeding through the breathing layer and taken out through plumbing assembly.
12. At last, after keeping the vacuum assembly in the running for 3 hours, then allowed to cure for next 7 hours.
13. This method employs vacuum bag to supply pressure at the time of the curing. Vacuum bags operate with a straightforward compression and allows the composite panel to cure.
14. Finishing: After taking out the panel, used sandpaper to make the surface smooth.

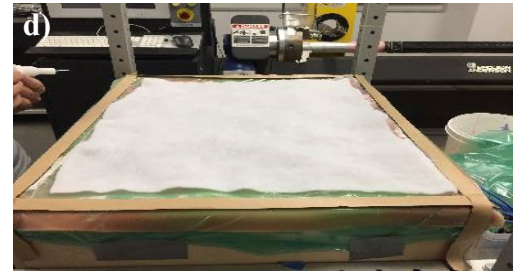
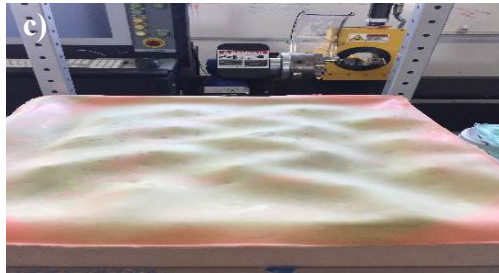
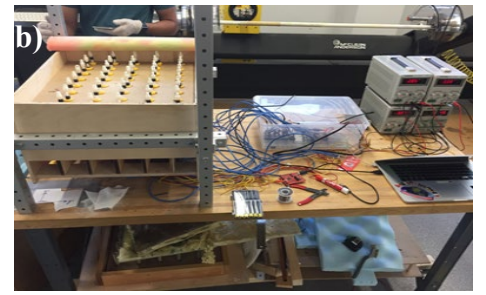


Figure 6.12 Production process of composite Architectural Panel a) Material Preparation b) Actuators and flexible membrane setting c) Actuators in motion d) Material Layup process e) Vacuum Bagging f) Vacuum processing g) Cured Composite panel h) Finished composite panel (Picture courtesy Gurjar)

The flexible membrane and density of the actuators array play a vital role in the precision of the produced panel.

Computer simulations process run to see how much identical is the surface of the panels in comparison to ideal 3D Rhino surface. We conducted computer simulation analysis Auto Desk Alia to get the actual deviation on the scanned panel samples.

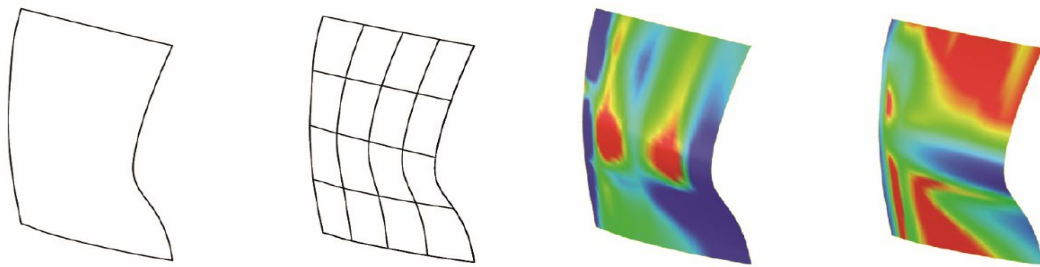


Figure 6.13 3-D Digital Evaluation (Ku)

6.2.4 Step 4 – Final Sample Testing and Analysis by Rhino and Auto Desk Alia

The curved panels scanned with the help of 3D Scanner in mesh form. Company name iSense.

1.a. Double Curve Structure

1. A scanned panel sample was overlapped using the Auto Desk Alia software with Rhino 3D, and the resulting mesh was analyzed with (+/-) 3.175 mm acceptance.
2. From the digital analysis, we found that 70 percent of the composite panel mesh was in line with the ideal Rhino structure as per Alia auto desk analysis. As shown in the figure, the green section indicates the part of the composite panel mesh that is with 70 percent accurate out of 100 percent, and the red/purple section shows the part of the mesh that varies from the

actual 3D structure.

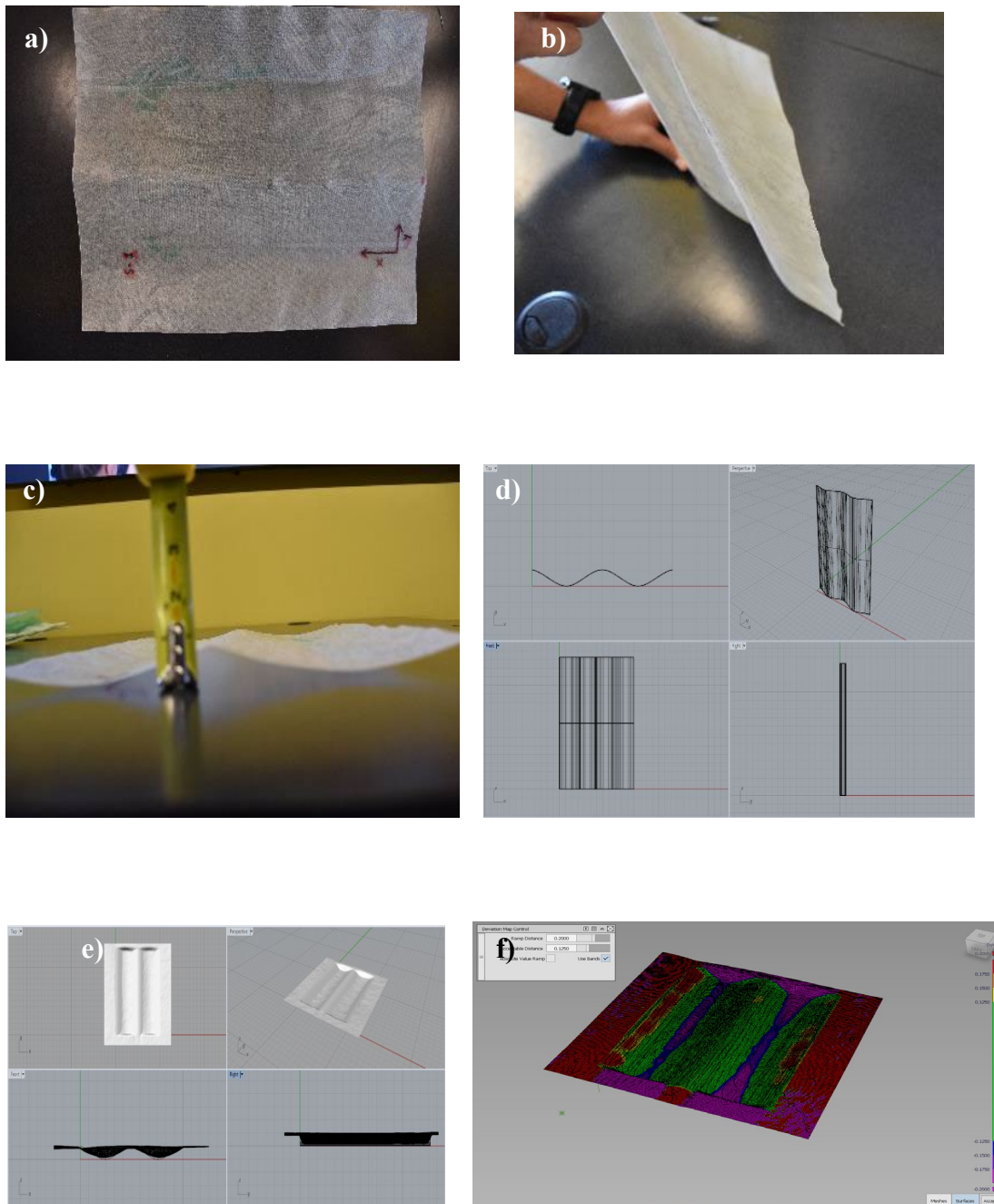
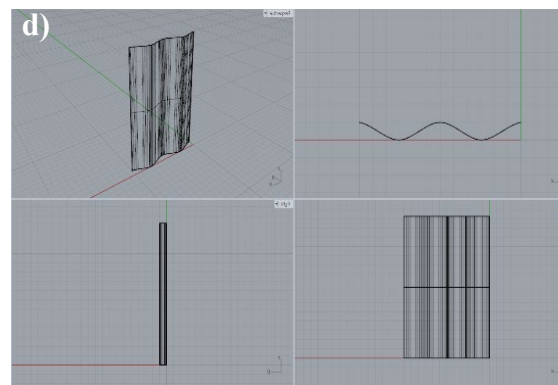
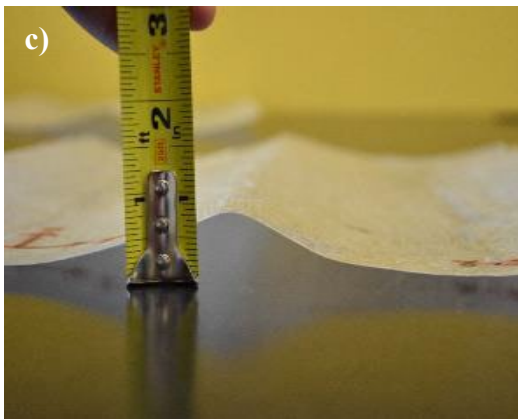


Figure 6.14. Double Curve Analysis using Rhino and Alias Auto Desk a) Double Curved front view b) Double Curved Side view, c) Cross sectional view, d) Rhino 3D structure, e) Scan sample in Rhino, f) Evaluation of scanned sample with ideal 3D structure. (Pictures courtesy Gurjar)

1.b. Double Curve Geometry

Description:

1. A scanned panel sample was overlapped using the Auto Desk Alia software with Rhino 3D, and the resulting mesh was analyzed with (+/-) 3.175 mm acceptance.
2. From the analysis, we found that 75 percent of the composite panel mesh was in line with the ideal Rhino structure as per Alia auto desk analysis. As shown in the figure 6.15(f) from Alia Auto desk, the green section indicates the part of the composite panel mesh that is with 75 percent accurate out of 100 percent, and the red/purple section shows the part of the mesh that varies from the actual 3D structure.



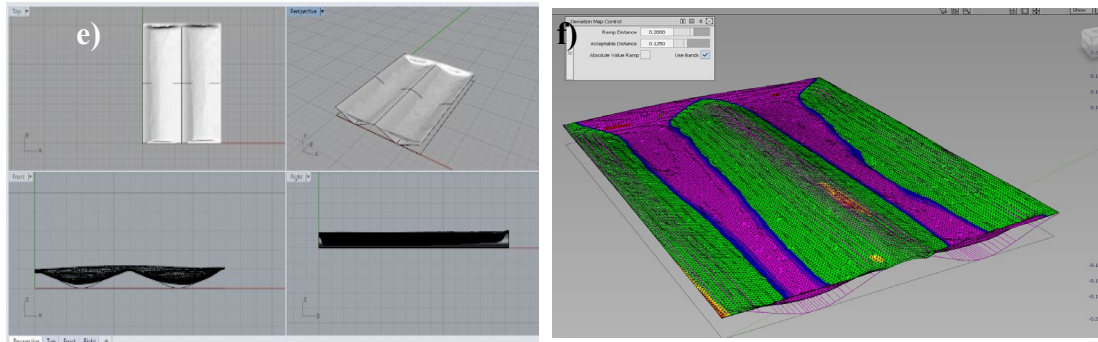


Figure 6.15. Double Curve Analysis using Rhino and Alias Auto Desk a) Double Curved front view b) Double Curved Side view, c) Cross sectional view, d) Rhino 3D structure, e) Scan sample in Rhino, f) Evaluation of scanned sample with ideal 3D structure. (Pictures courtesy Gurjar)

1.c. Double Curve Geometry

Description:

1. A scanned panel sample was overlapped using the Auto Desk Alia software with Rhino 3D, and the resulting mesh was analyzed with (+/-) 3.175 mm acceptance.
2. From the analysis, we found that 60 percent of the composite panel mesh was in line with the ideal Rhino structure as per Alia auto desk analysis. As shown in the figure 6.16(f), the green section indicates the part of the composite panel mesh that is with 60 percent accurate out of 100 percent, and the red/purple section shows the part of the mesh that varies from the actual 3D structure.

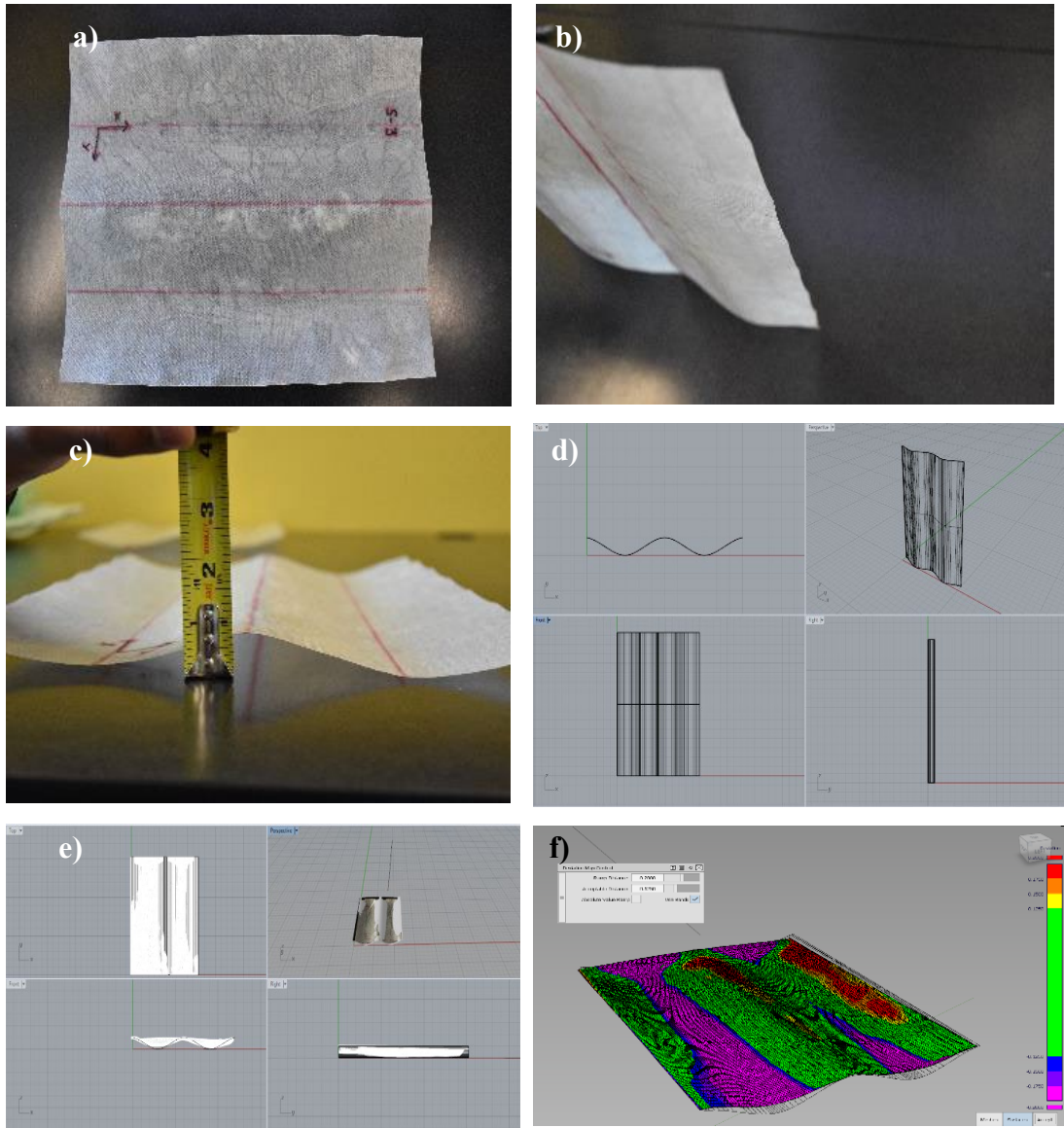


Figure 6.16. Double Curve Analysis using Rhino and Alias Auto Desk a) Double Curved front view b) Double Curved Side view, c) Cross sectional view, d) Rhino 3D structure, e) Scan sample in Rhino, f) Evaluation of scanned sample with ideal 3D structure. (Pictures courtesy Gurjar)

2.a. Concave Geometry

Description:

1. A scanned panel sample was overlapped using the Auto Desk Alia software with Rhino 3D, and the resulting mesh was analyzed with (+/-) 3.175 mm

acceptance.

- From the analysis, we found that 40 percent of the composite panel mesh was in line with the ideal Rhino structure as per Alia auto desk analysis. As shown in the figure, the green section indicates the part of the composite panel mesh that is 40 percent accurate out of 100 percent, and the red/purple section shows the part of the mesh that varies from the actual 3D structure.

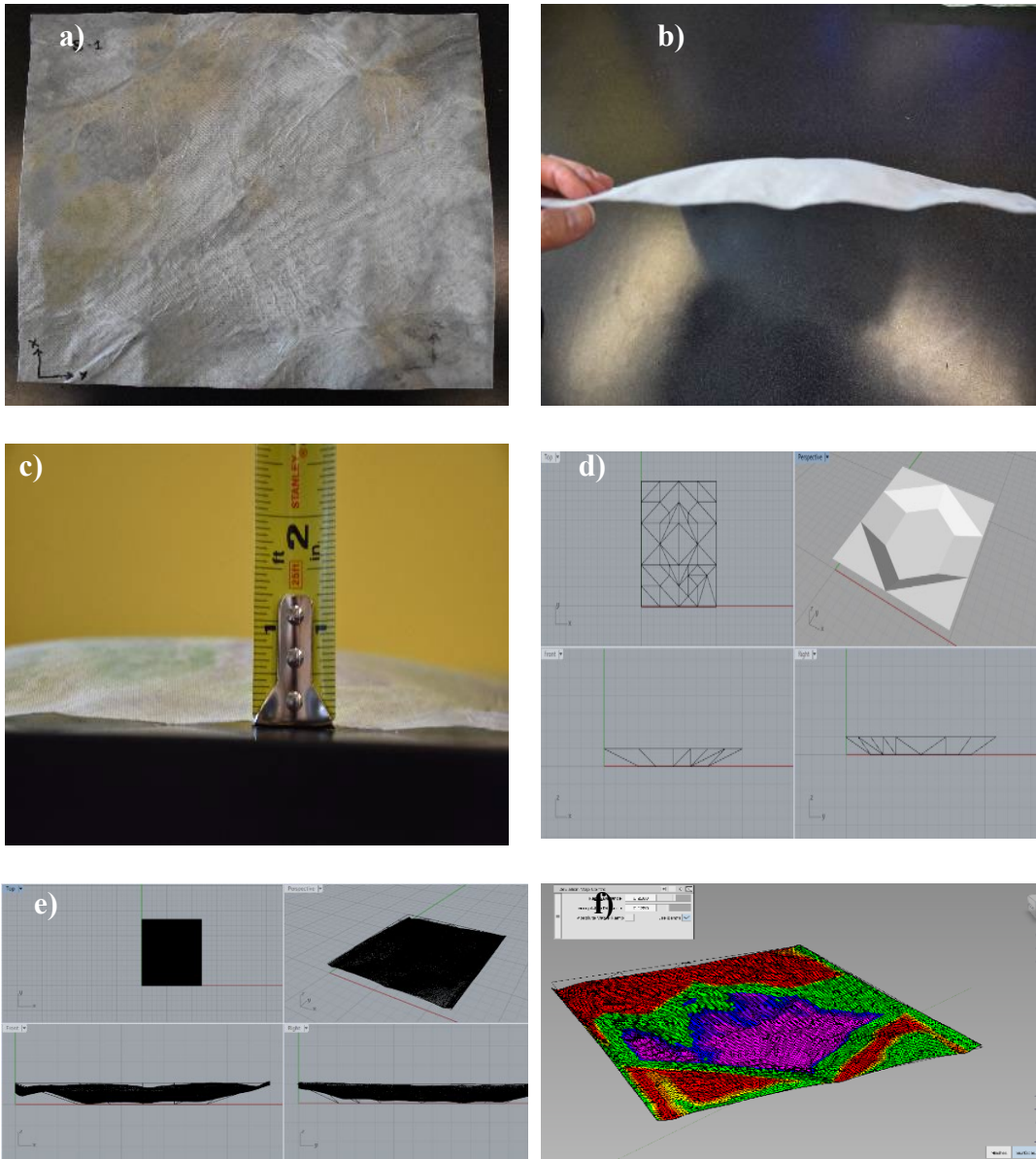
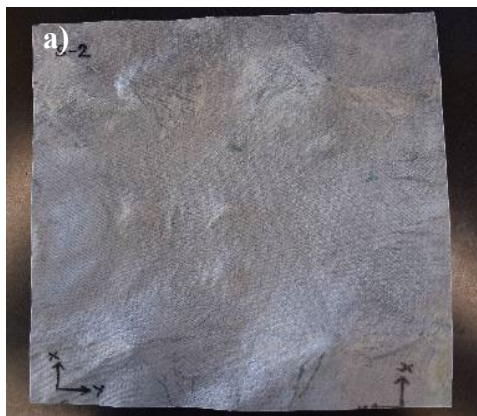


Figure 6.17. Concave Curve Analysis using Rhino and Alias Auto Desk a) Concave Curved front view b) Concave Curved Side view, c) Cross sectional view, d) Rhino 3D structure, e) Scan sample in Rhino, f) Evaluation of scanned sample with ideal 3D structure. (Pictures courtesy Gurjar)

2.b. Concave Geometry

Description:

1. A scanned panel sample was overlapped using the Auto Desk Alia software with Rhino 3D, and the resulting mesh was analyzed with (+/-) 3.175 mm acceptance.
2. From the analysis, we found that 65 percent of the composite panel mesh was in line with the ideal Rhino structure as per Alia auto desk analysis. As shown in the figure, the green section indicates the part of the composite panel mesh 65 percent accurate out of 100 percent, and the red/purple section shows the part of the mesh that varies from the actual 3D structure.



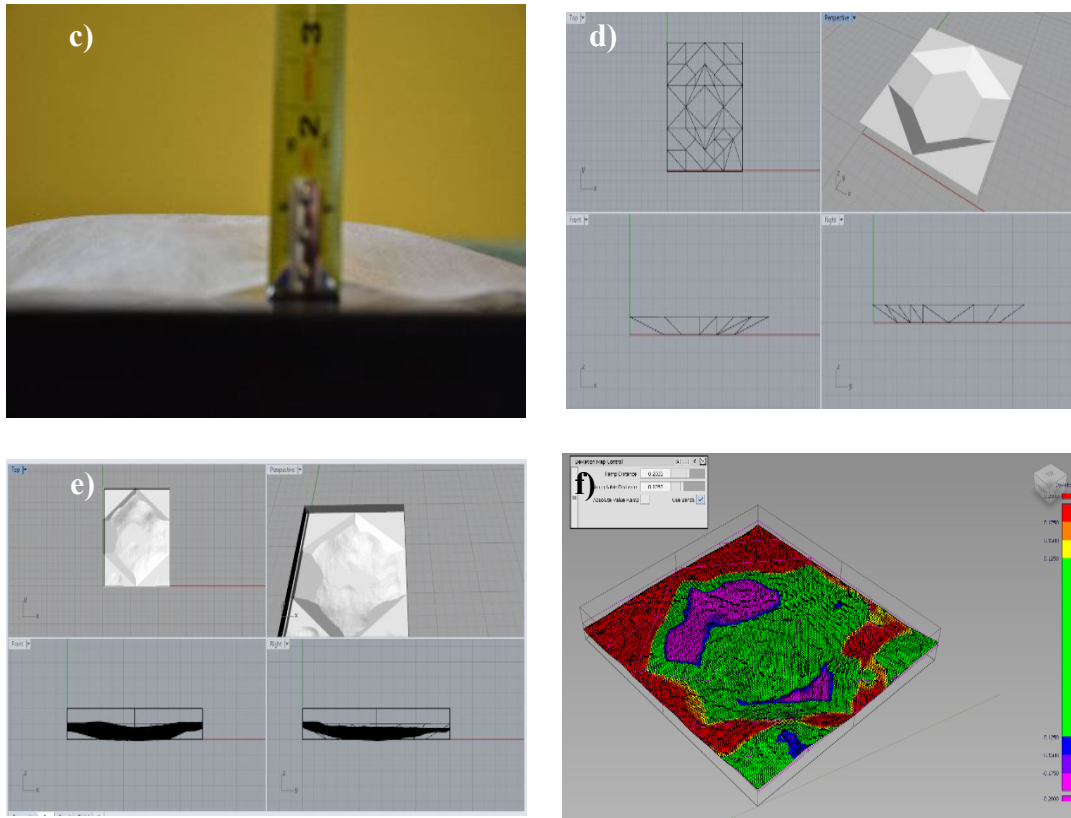


Figure 6.18. Concave Curve Analysis using Rhino and Alias Auto Desk a) Concave Curved front view b) Concave Curved Side view, c) Cross sectional view, d) Rhino 3D structure, e) Scan sample in Rhino, f) Evaluation of scanned sample with ideal 3D structure. (Pictures courtesy Gurjar)

2.c. Concave Geometry

Description:

1. A scanned panel sample was overlapped using the Auto Desk Alia software with Rhino 3D, and the resulting mesh was analyzed with (+/-) 3.175 mm acceptance.
2. From the analysis, we found that 65 percent of the composite panel mesh was in line with the ideal Rhino structure as per Alia auto desk analysis. As shown in the figure, the green section indicates the part of the composite panel mesh

65 percent accurate out of 100 percent, and the red/purple section shows the part of the mesh that varies from the actual 3D structure.

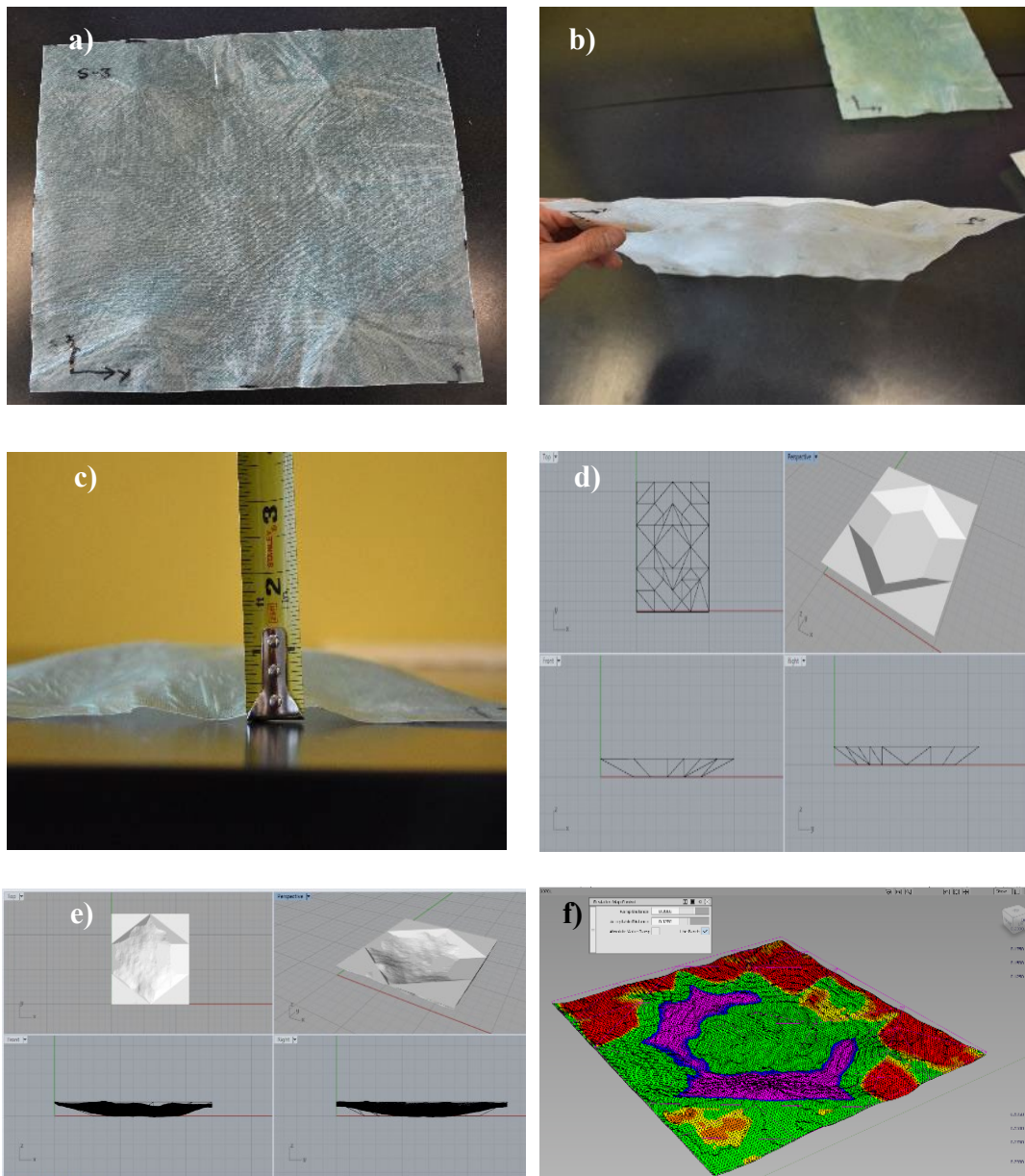
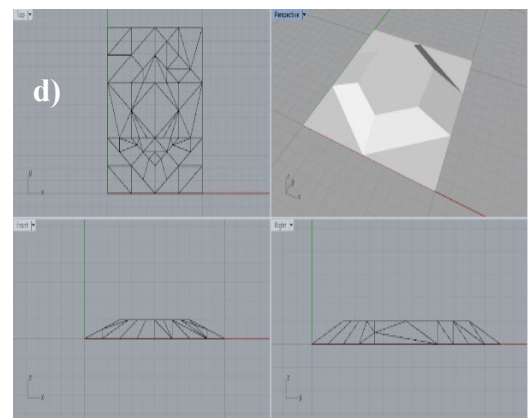
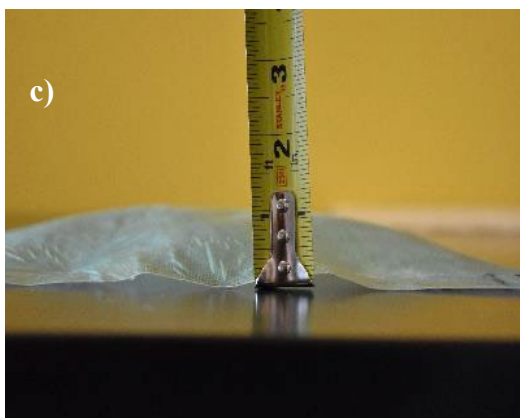
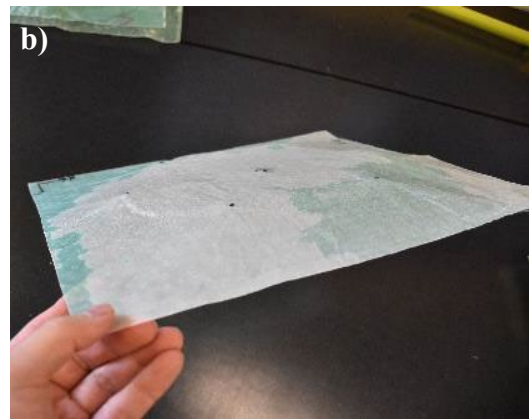
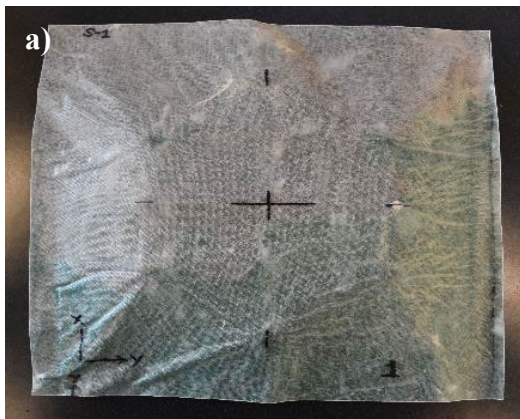


Figure 6.19. Concave Curve Analysis using Rhino and Alias Auto Desk a) Concave Curved front view b) Concave Curved Side view, c) Cross sectional view, d) Rhino 3D structure, e) Scan sample in Rhino, f) Evaluation of scanned sample with ideal 3D structure. (Pictures courtesy Gurjar)

3. a. Convex Geometry

Description:

1. A scanned panel sample was overlapped using the Auto Desk Alia software with Rhino 3D, and the resulting mesh was analyzed with (+/-) 3.175 mm acceptance.
2. From the analysis, we found that 40 percent of the composite panel mesh was in line with the ideal Rhino structure as per Alia auto desk analysis. As shown in the figure, the green section indicates the part of the composite panel mesh 40 percent accurate out of 100 percent, and the red/purple section shows the part of the mesh that varies from the actual 3D structure.



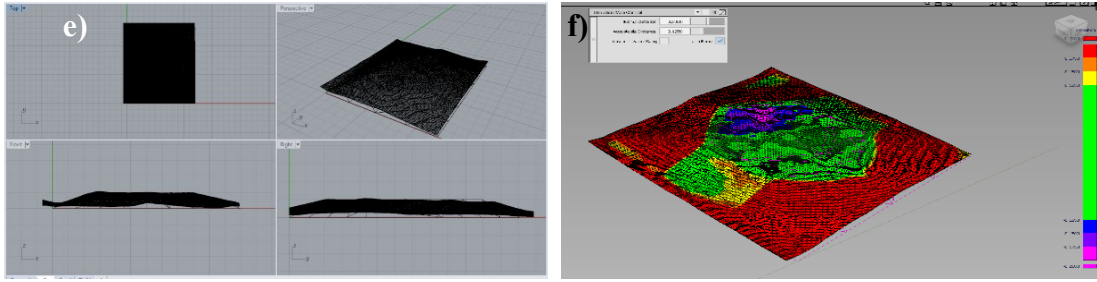
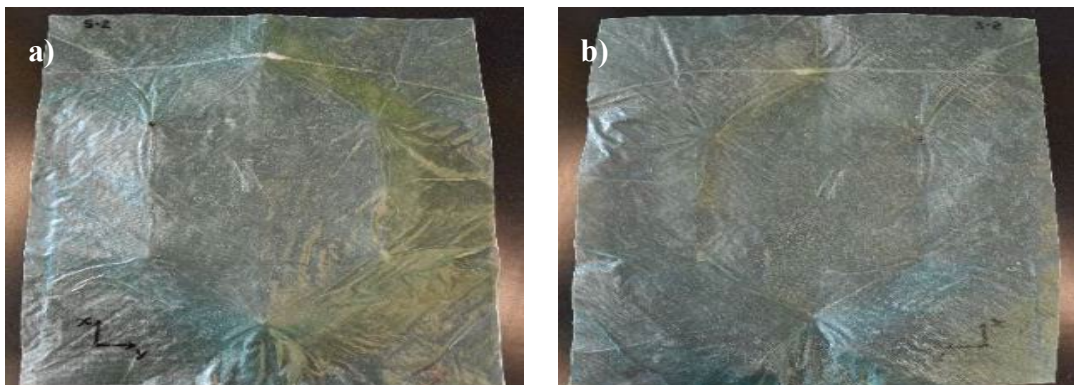


Figure 6.20. Convex Curve Analysis using Rhino and Alias Auto Desk a) Convex Curved front view b) Convex Curved Side view c) Convex Curved Back view d) Side View, e) Rhino 3D structure, f) Scan sample in Rhino, g) Evaluation of scanned sample with ideal 3D structure. (Pictures courtesy Gurjar)

3.b. Convex Geometry

Description:

1. A scanned panel sample was overlapped using the Auto Desk Alia software with Rhino 3D, and the resulting mesh was analyzed with (+/-) 3.175 mm acceptance.
2. From the analysis, we found that 55 percent of the composite panel mesh was in line with the ideal Rhino structure as per Alia auto desk analysis. As shown in the figure, the green section indicates the part of the composite panel mesh 55 percent accurate out of 100 percent, and the red/purple section shows the part of the mesh that varies from the actual 3D structure.



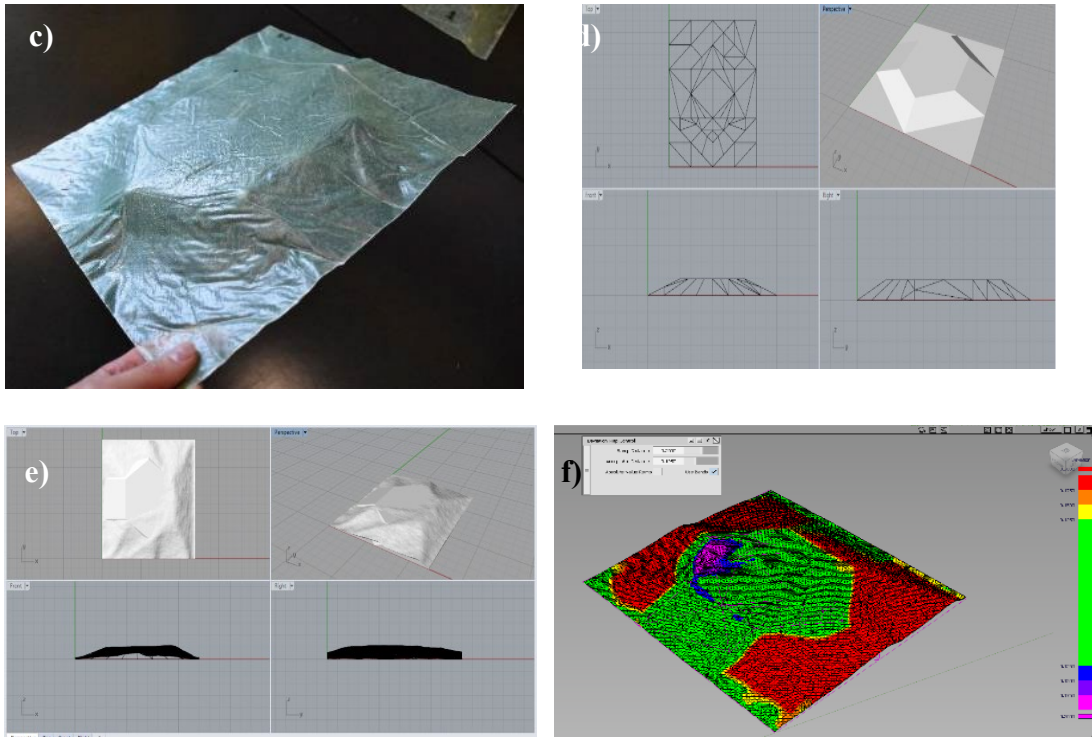
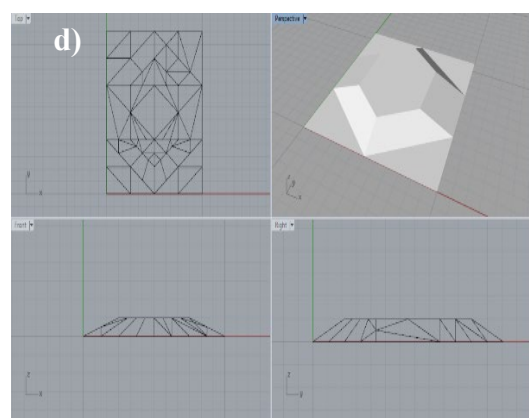
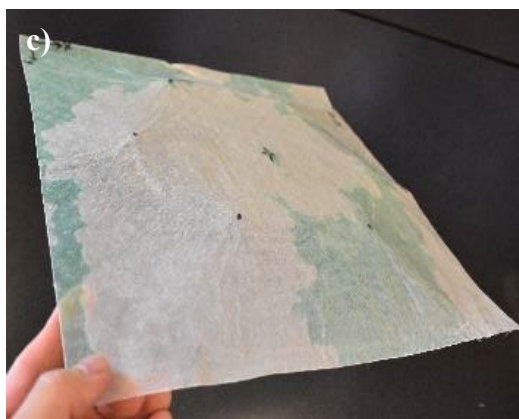


Figure 6.21. Convex Curve Analysis using Rhino and Alias Auto Desk a) Convex Curved front view b) Convex Curved Back view c) Convex Curved Side view d) Rhino 3D structure, e) Scan sample in Rhino, f) Evaluation of scanned sample with ideal 3D structure. (Pictures courtesy Gurjar)

c. Convex Geometry

Description:

1. A scanned panel sample was overlapped using the Auto Desk Alia software with Rhino 3D, and the resulting mesh was analyzed with (+/-) 3.175 mm acceptance.
2. From the analysis, we found that 65 percent of the composite panel mesh was in line with the ideal Rhino structure as per Alia auto desk analysis. As shown in the figure, the green section indicates the part of the composite panel mesh 65 percent accurate out of 100 percent, and the red/purple section shows the part of the mesh that varies from the actual 3D structure.



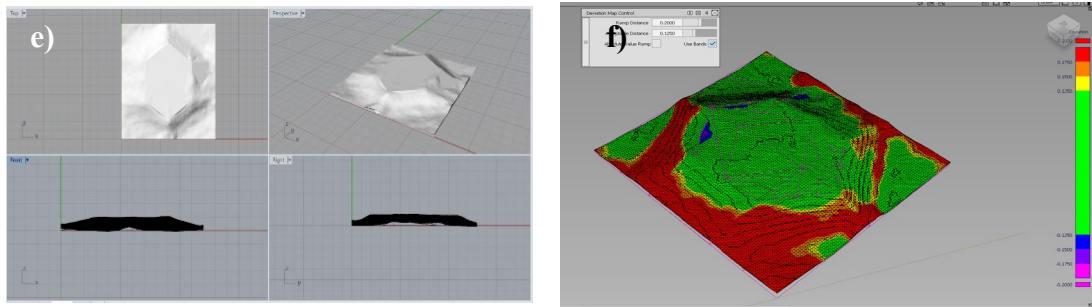


Figure 6.22. Convex Curve Analysis using Rhino and Alias Auto Desk a) Convex Curved front view b) Convex Curved Back view c) Convex Curved Side view d) Rhino 3D structure, e) Scan sample in Rhino, f) Evaluation of scanned sample with ideal 3D structure. (Pictures courtesy Gurjar)

4. a. Freeform Geometry

Description:

1. A scanned panel sample was overlapped using the Auto Desk Alia software with Rhino 3D, and the resulting mesh was analyzed with (+/-) 3.175 mm acceptance.
2. From the analysis, we found that 40 percent of the composite panel mesh was in line with the ideal Rhino structure as per Alia auto desk analysis. As shown in the figure, the green section indicates the part of the composite panel mesh 40 percent accurate out of 100 percent, and the red/purple section shows the part of the mesh that varies from the actual 3D structure.

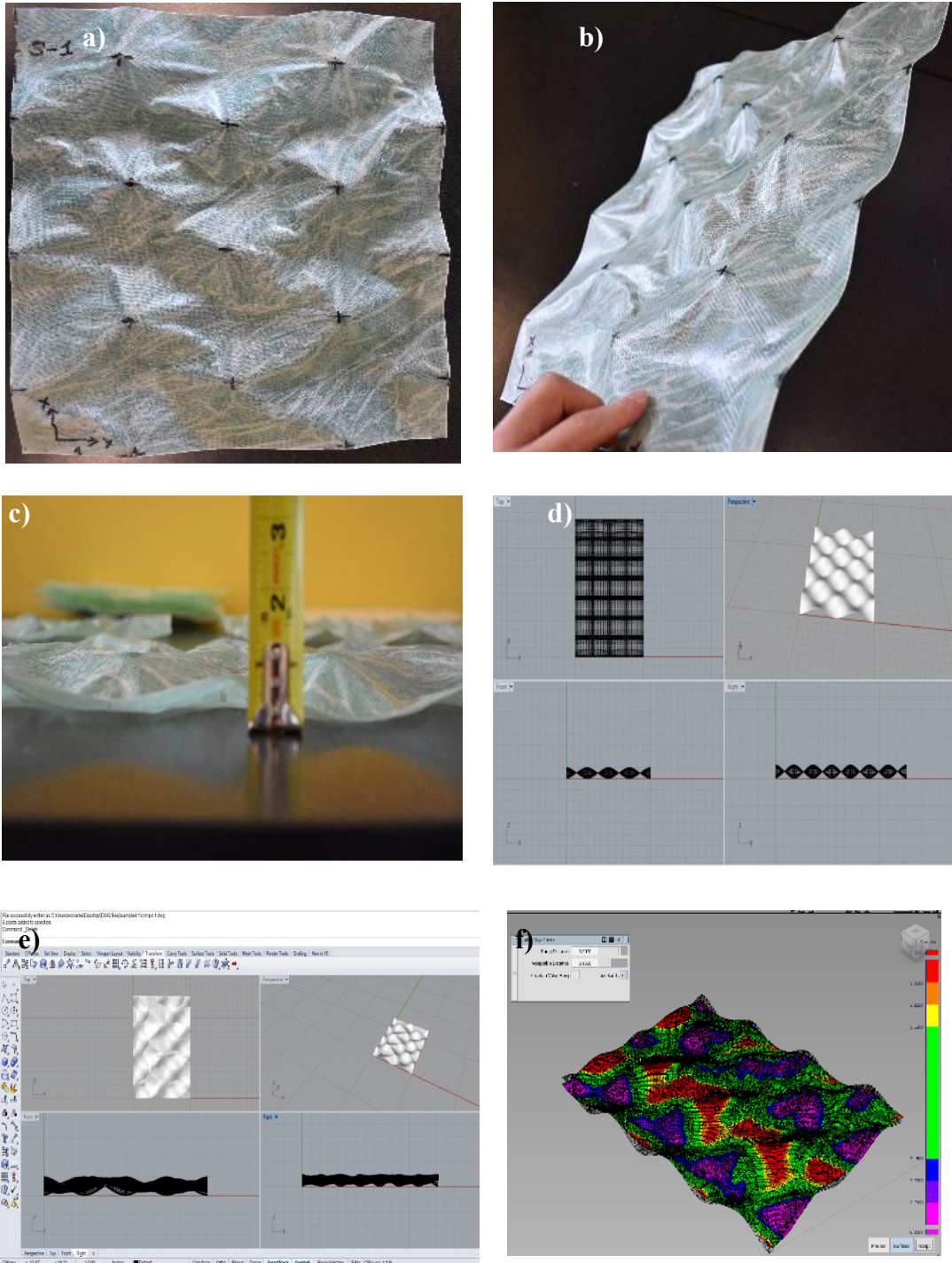
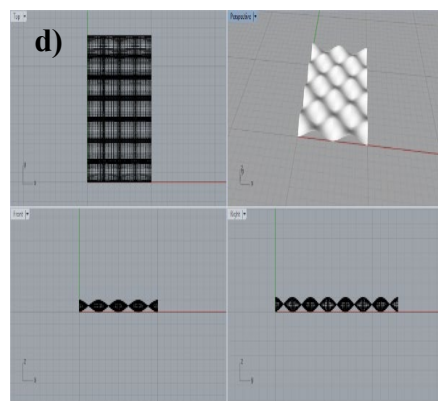
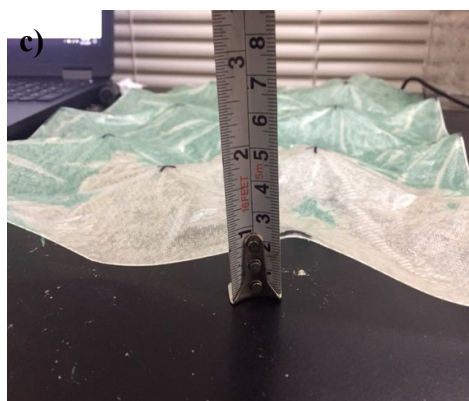
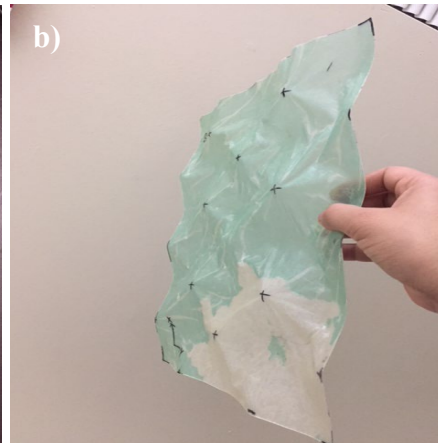


Figure 6.23. Freeform Curve Analysis using Rhino and Alias Auto Desk a) Freeform front view b) Freeform Side view c) Freeform cross section view d) Rhino 3D structure, e) Scan sample in Rhino, f) Evaluation of scanned sample with ideal 3D structure. (Pictures courtesy Gurjar)

4.b. Freeform Geometry

Description:

1. A scanned panel sample was overlapped using the Auto Desk Alia software with Rhino 3D, and the resulting mesh was analyzed with (+/-) 3.175 mm acceptance.
2. From the analysis, we found that 30 percent of the composite panel mesh was in line with the ideal Rhino structure as per Alia auto desk analysis. As shown in the figure, the green section indicates the part of the composite panel mesh 30 percent accurate out of 100 percent, and the red/purple section shows the part of the mesh that varies from the actual 3D structure.



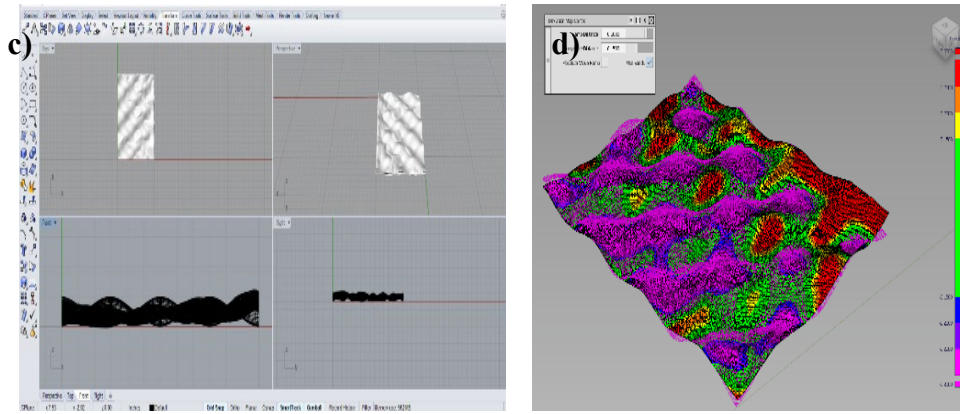


Figure 6.24. Freeform Curve Analysis using Rhino and Alias Auto Desk a) Freeform front view b) Freeform Side view c) Freeform cross section view d) Rhino 3D structure, e) Scan sample in Rhino, f) Evaluation of scanned sample with ideal 3D structure. (Pictures courtesy Gurjar)

4.c. Freeform Geometry

Description:

1. A scanned panel sample was overlapped using the Auto Desk Alia software with Rhino 3D, and the resulting mesh was analyzed with (+/-) 3.175 mm acceptance.
2. From the analysis, we found that 40 percent of the composite panel mesh was in line with the ideal Rhino structure as per Alia auto desk analysis. As shown in the figure, the green section indicates the part of the composite panel mesh 40 percent accurate out of 100 percent, and the red/purple section shows the part of the mesh that varies from the actual 3D structure.

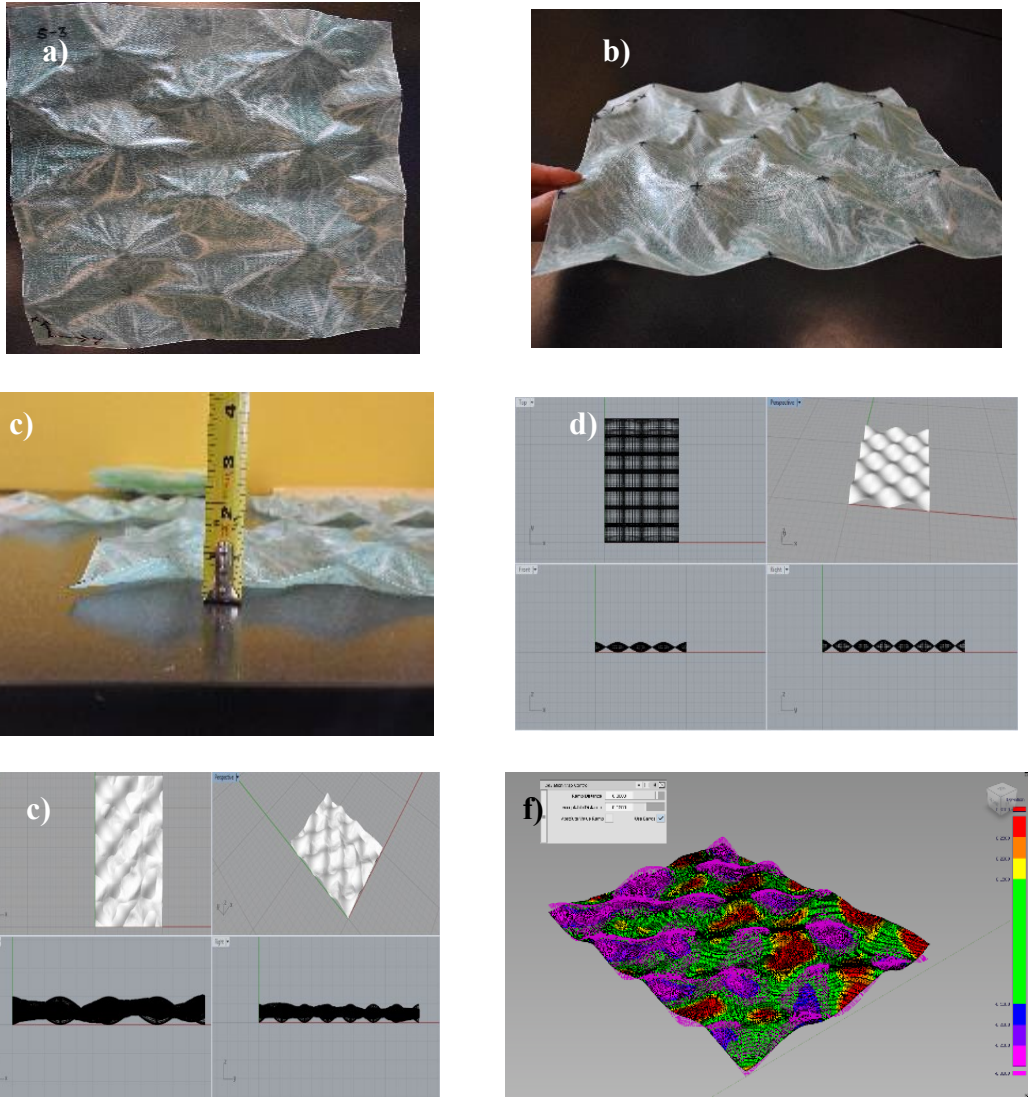


Figure 6.25. Freeform Curve Analysis using Rhino and Alias Auto Desk a) Freeform front view b) Freeform Side view c) Freeform cross section view d) Rhino 3D structure, e) Scan sample in Rhino, f) Evaluation of scanned sample with ideal 3D structure. (Pictures courtesy Gurjar)

6.3 Results and Discussion

The deviations of the different samples are varying as per their complexity of the structure. The data collected was analyzed by the outlier formula and no outlier was found in the collected data. For reference please see appendix A. It shows that the collected data of the different structures was without outliers.

In this research, samples were produced with four different curves by using flexible surface mold. The height of the actuator forming the mold curvature was limited to zero mm low and 25.4 mm high in shape of the curvature. Each curvature within the sample was obtained by each set of four actuators. The deviation from ideal geometry seen in this experiment was designed to observe the effect of curves on the samples. In this analysis, data of the actual heights was collected and analyzed at individual curve within the samples. Comparison between ideal and actual geometry shows that, most of the discrepancies occur between up and down actuators which resist the flexible membrane to stretch or freely drape between the specific curve and create uneven curvature on the panels. Which can be resolved by using Liner servo actuators in future work, so the height can vary within the up and down limit to reduce discrepancies of the different curves. The results were depicted in the line graph for analyzing the curves for different shape of panel by comparing to the ideal geometry.

In Figure 6.25 it shows five different arrays consisting of eight different actuators. In double curved geometry 24 actuators were raised to a height of 25.4 mm and 16 were at zero mm height as per ideal 3 D surface geometry forming a total of 40. The average observed heights of the curve at 24 high actuators was 19.06 mm whereas the average observed height of the remaining low actuators was 0.85 mm, which was within the range of allowable standard deviation. To see a more detailed account of

the actuators, refer to Appendix B.

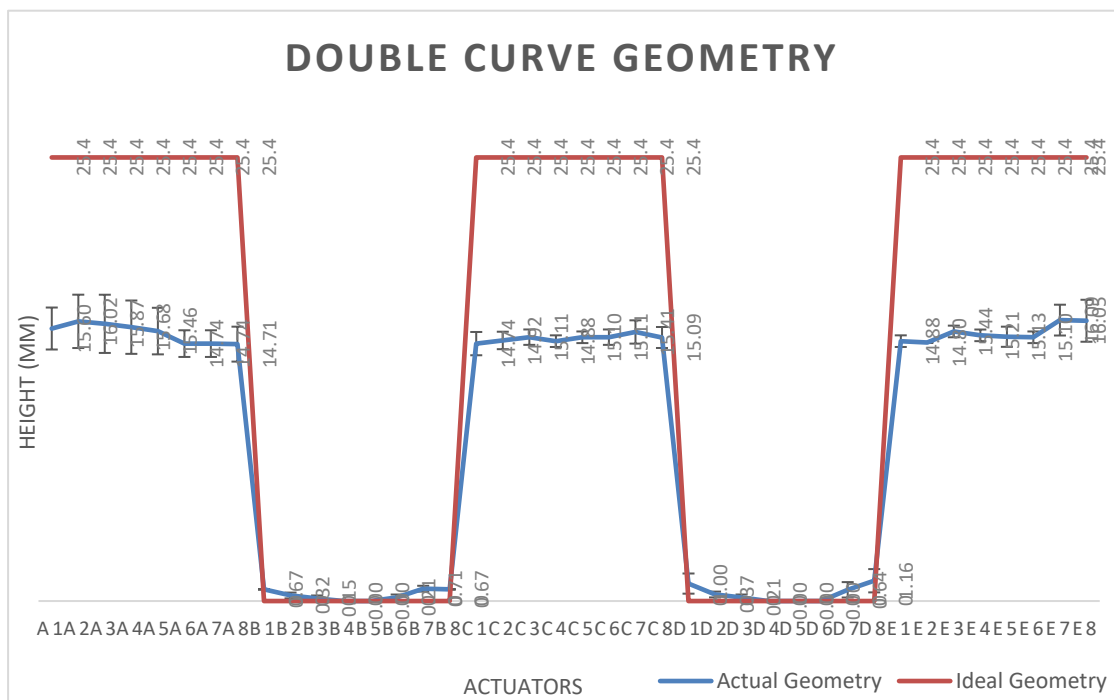


Figure 6.26. Double curve geometry comparison of ideal versus actual at individual actuator

In Figure 6.26 it shows five different arrays consisting of seven actuators each. In Concave curved geometry 24 actuators were raised to a height of 25.4 mm and 11 were at zero mm height as per ideal 3D surface geometry forming a total of 35 for maintain the even geometry of the panel. The average observed heights of the curve at 24 high actuators was 22.28 mm whereas the average observed height of the remaining 11 low actuators was 6.2 mm, which was within the range of allowable standard deviation and produced concave curved panel. To see a more detailed account of the actuators, refer to Appendix B.

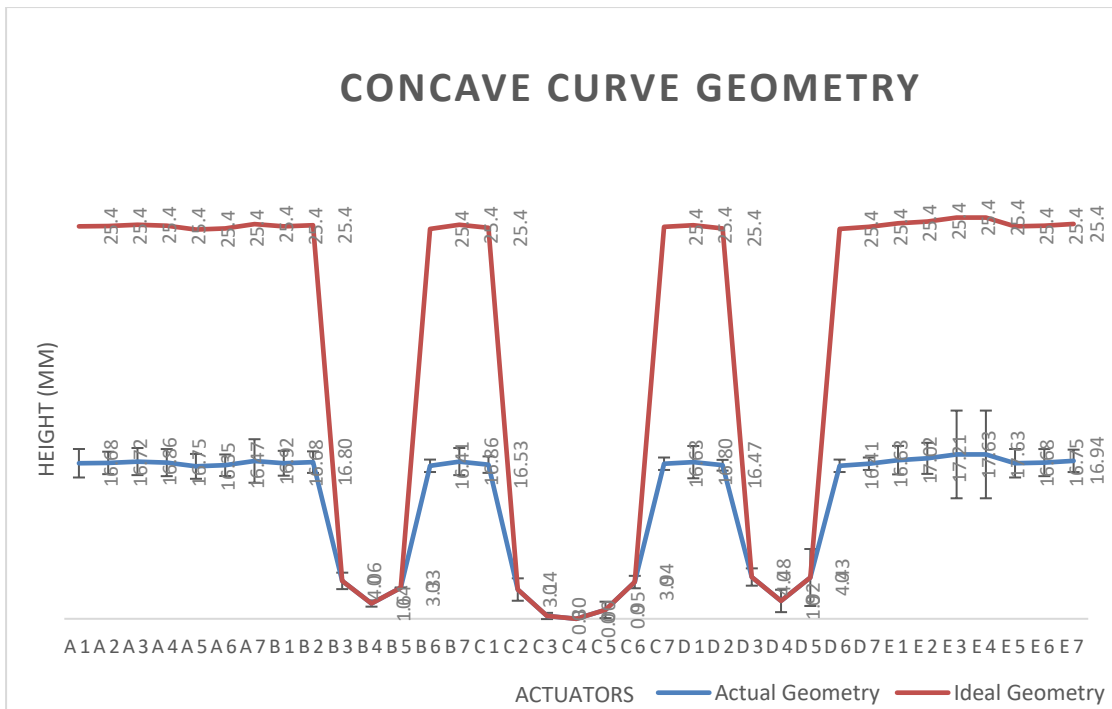


Figure 6.27. Concave curve geometry comparison of ideal versus actual at individual actuator

In Figure 6.27, it shows five different arrays consisting of seven actuators each. In Convex curved geometry 11 actuators were raised to a height of 25.4 mm and 24 were at zero mm height as per ideal 3D surface geometry forming a total of 35 for maintain the even geometry of the panel. The average observed heights of the curve at 11 high actuators was 21.29 mm whereas the average observed height of the remaining 24 low actuators was 2.74 mm, which was within the range of allowable standard deviation and produced convex curved panel. To see a more detailed account of the actuators, refer to Appendix B.

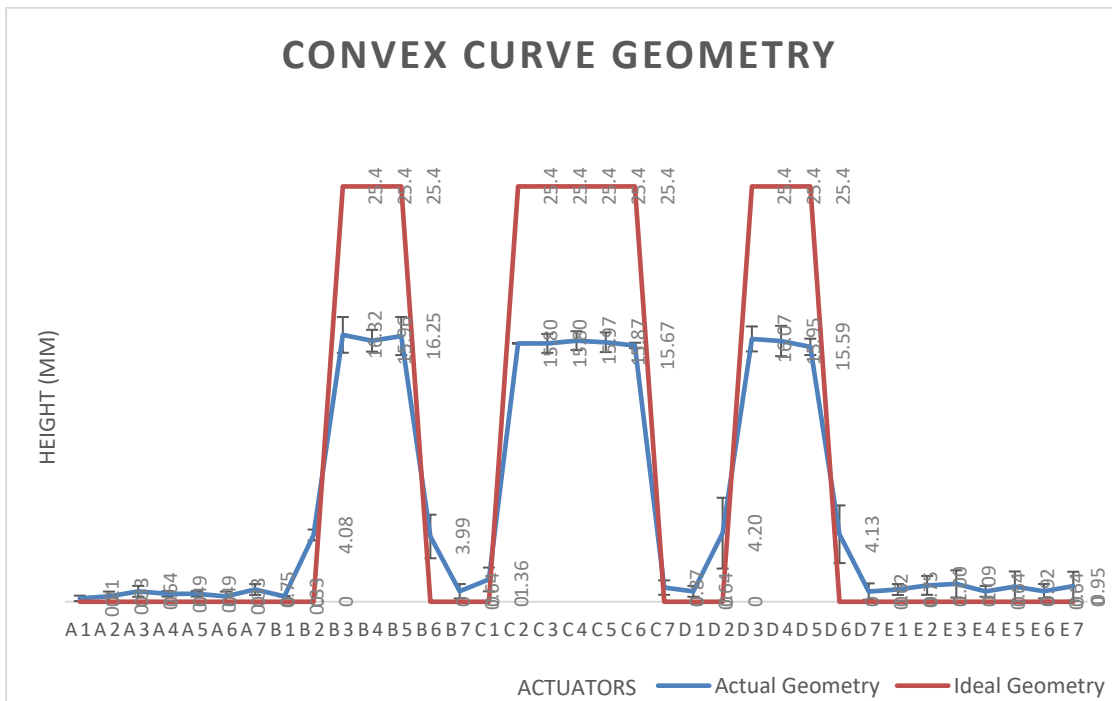


Figure 6.28. Convex curve geometry comparison of ideal versus actual at individual actuator

In Figure 6.28 it shows five different arrays consisting of eight different actuators. In Freeform curved geometry 20 actuators were raised to a height of 25.4 mm and 20 were at zero mm height as per ideal 3D surface geometry forming a total of 40. The average observed heights of the curve at 20 high actuators was 21.58 mm whereas the average observed height of the remaining 20 low actuators was 2.13 mm, which was within the range of allowable standard deviation. To see a more detailed account of the actuators, refer to Appendix B.

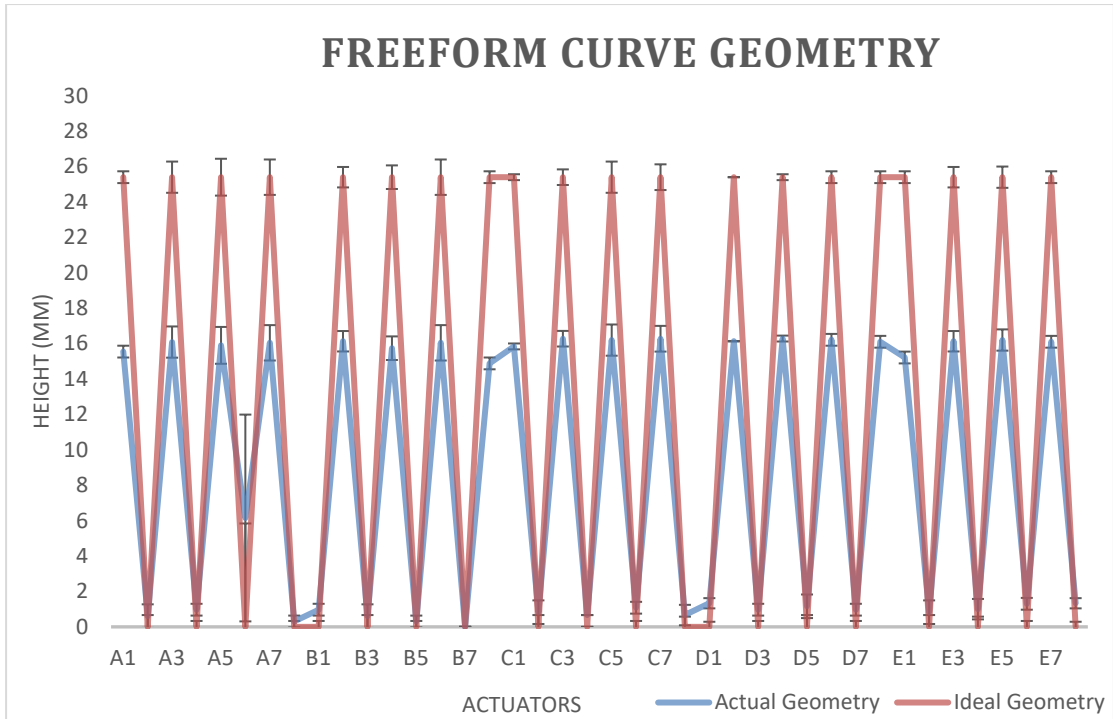


Figure 6.29. Freeform curve geometry comparison of ideal versus actual at individual actuator

P-Value

Goal First: Samples are repeatable in same shape

P- value for sample geometry comparison with same geometry samples:

In the output, it can be observed that within the same shape of the curved panel samples are significant because both of their p-values less than common alpha level of 0.05. then we reject the null hypothesis. Thus, the data is statically significant. For more details refer to Appendix C.

Goal Second: Samples are same as ideal 3-D design

P- value for actual observed geometry and ideal curve geometry for all the different shapes:

In the output of actual geometry Vs ideal geometry, it can be observed that average of all the samples Vs ideal shape structure of the curved panel are not significant because both of their p-values less than common alpha level of 0.05. Thus, the data of actual geometry Vs ideal geometry is statically not significant. For more details refer to Appendix C.

By studying P value and F value for first goal, it was conclude that the goal of manufacturing of architectural panels on the prototype was achieved and the manufactured samples were able to reproduce, which proven that the proof of concept of prototype was working.

By studying P and F value for second goal, where the ideal geometry of the 3-d structure was compared to the averages of actual observed samples. It concludes that in order to get the exact replication of the 3-d design needs further recommended work on the prototype.

The discrepancies are due to the motion of actuators is limited to upper limit 25.4 mm to lower limit 0 mm. When the 3-dimensional structure in software is transformed to one dimensional which in turn make the porotype flexible surface into 3-dimension geometry. The actuator moves up and down to the programmed setting but as the membrane is flexible, the actuator was able to move accordingly and were able to form a curvature geometry. The discrepancy occurred in curvature because there was no supporting aid between the two upper and lower moving actuators, which caused flexible surface to drape and create discrepancies. The discrepancies can be reduced by increasing the density of actuators by using linear servo actuator. We can vary the

height of actuator at each point which reflect the better flow in the curvature and the obtain the actual curvature of the 3-Dimensional structure.

7. CONCLUSION

From the theoretical and practical work on a prototype, the following conclusions are drawn:

The manufacturing of curved composite panel is possible through the use of the automated flexible mold system. An experimental approach is the best way to automate the molding process to curb the mold wastage, remove the mold making process and use of composite material in structural panels. Few experiments were conducted to understand the deviation of the scanned physical structure from the digital geometry of the curved panel.

One of the technical problems that arose was the tip of actuator started making some dimples on the flexible surface which were transferred to composite panels. As the control on the flexible surface was not attainable, we faced minor deviation on the surface of the panel.

In this process, we were bound to give constant power supply to the actuators DC motor until the process of vacuum bagging was complete which caused actuators to burn out. Also, the vacuum bagging created a high vacuum on top of actuator heads. Compression on the head of actuators caused a slight variation in the surface of the panel leading to the loss of actual geometry. Some actuators jammed occasionally and burned out, especially during the production. Except these no major complications occurred during the manufacturing process of the architectural panel. By this prototype, we demonstrated the manufacturing of curved panels of 38.1 cm × 30.48 cm and thickness of around 0.5842 mm thickness. Panels can be assembled which is sufficient to form freely formed building shapes. According to the experiments conducted on the different shapes, the manufacturing of architectural panels on the prototype was achieved and the manufactured samples were able to reproduce, which

proven that the proof of concept of prototype was working, which conclude that first goal of creating working prototype is achieved and the samples can be reproducible in the same shape and geometry with minimal tolerance limit.

The conclusion of the second goal was to replicate the ideal 3-d design into actual samples was not fully achieved, it can be said that optimizing the prototype parameters, process parameters and parameters for complex shapes is a challenge that needs to be further researched with keeping all the recommended future work, so that exact replica of the ideal 3-d structures can be developed on flexible mold. It can be assumed that these problems will be overcome as a reaction to even greater pressure on the industry to allow for greater product variety, flexibility in production and lower tooling costs. The impact on the making of smaller structural surfaces will undoubtedly be felt. The main advantages of this technique are the low costs and the simplicity of the mold in comparison to CNC made static molds which are restricted to specific geometry and not able to reconfigure in different composite panel shapes. This process allows product to be developed in less time and fewer steps. The use of computer-controlled actuators allows more efficient and better controlled on 3D surfaces which is the current need and can be achieved by assimilating textile composites in facade industry.

8. RECOMMENDATIONS FOR FURTHER RESEARCH

The method presented in this paper involves using sparsely arranged actuators. The use of higher density of actuators, which would, in turn, lead to a construction of panels close to its digital design. The construction of the composite panels is not restricted to only one type of material. We can look for other available materials. Instead of using DC motor actuator use the height varying Linear Servos so it would be in more controlled heights. This is because there will not be any constraint on the motion of the actuator.

In next step, we can create different panels of different thickness. We can manipulate the thickness of the flexible membrane to get even and smoother surface of the composite panel. By changing the spring assembly of the male mold with Linear servo actuators in reverse of the body shape will also give a better definition to the composite panel. When the panel is easily achievable next step would be introducing the polystyrene, and make the sandwich structures by assembling panels. In future work geometries can be achieved more defined and smooth in by working on all these stated points below:

- Frame work of prototype structure
- Height of actuators because of vacuum bagging process
- Thickness of the Flexible membrane
- Density of actuators
- Replacing DC motor actuators with Height varying liner servo actuators.

9. REFERENCES

2016. 16 April 2017. <<http://support.minitab.com/en-us/minitab-express/1/help-and-how-to/modeling-statistics/regression/how-to/multiple-regression/interpret-the-results/all-statistics-and-graphs/#vif>>.
- American Society for Testing and Materials . *Standard Test Method for Bursting Strength of Fabrics Constant-Rate-of-Extension (CRE) Ball Burst Test*. American Society for Testing and Materials , 2013.
- Bechthold, Martin. *Innovative Surface Structures - Technologies and Applications*. Abingdon: Taylor and Francis , 2008.
- . *Innovative Surface Structures - Technologies and Applications*. Abingdon, Oxon: Tyler and Francis, 2008.
- Boers, S.H.A. *Optimum forming strategies with a 3D reconfigurable die*. Eindhoven, The Netherlands: Eindhoven : Technische Universiteit Eindhoven, 2006.
- Campbell, F.C. "Structural Composite Materials." *ASM International* (2010): 1-30.
- Casillas, Roy , et al. 18 January 2018. <http://faculty.arch.tamu.edu/media/cms_page_media/4433/TWATerminal.pdf>.
- Corazza et al., Marco. *Fiber Composite Fabrication: Experimental Methods of Architectural Applications*. London, 2014.
- Daan Rietbergen, et al. *Adjustable Mould For Architectural Applications*. Delft, 2010.
- Dhande and Rao. "A flexible surface tooling for sheet-forming processes: conceptual studies and numerical simulation." *Journal of Materials Processing Technology* 124 (2002): 133-143.
- Gehry, Frank. *A major architectural gesture*. n.d. 18 January 2018. <<http://www.fondationlouisvuitton.fr/en/la-fondation/un-geste-architectural-majeur.html>>.
- Groeneveld, H. D. "DEFORMATION CONTROL IN EXPLOSIVE FORMING." *The IX International Symposium on Explosive Production of New Materials*:. Ed. A. Deribas and Yu. Scheck. Moscow, Russia: TORUS PRESS Ltd, 2008. 51.
- Kleespies, H.S. and R.H. Crawford. "Vacuum Forming of Compound Curved." *Journal of Manufacturing System* Vol 17/No. 5 (1988): 325-337.
- Lauchhammer Bio Towers*. n.d. 18 January 2018. <<https://www.open-iba.de/en/geschichte/2000-2010-iba-furst-puckler-land/bioturme-lauchhammer/>>.
- Lee, Ghang and Seonwoo Kim. "Case Study of Mass Customization of Double-Curved Metal Façade Panels Using a New Hybrid Sheet Metal Processing

- Technique." *JOURNAL OF CONSTRUCTION ENGINEERING AND MANAGEMENT* (NOVEMBER 2012): 1322-1330.
- Mazumdar, Sanjay K. "Composites manufacturing : materials, product, and process." CRC PRESS, 2002.
- . *COMPOSITES MANUFACTURING Materials, Product, and Process Engineering*. Boca Raton: CRC Press LLC, 2002.
- Mercedes-Benz. *Architecture*. n.d. 18 January 2018. <<https://www.mercedes-benz.com/en/mercedes-benz/classic/museum/architecture/>>.
- Montgomery, et al. "Design Of Eperiments with Several Factors." Montgomery et, al. *Applied Statistic and Probablity for Engineers*. 2011. 553. John Wiley & Sons, Inc.
- Muwanga, Christina. *South Africa : a guide to recent architecture*. London: Ellipsis : Könemann, 1998.
- Nakajima, Naomasa. "A Newly Developed Technique to Fabricate Complicated Dies and Electrodes with Wires." *Bulletin of JSME* (1969): 1546-1554.
- Oesterle, S et al. "Zero Waste Free-Form Formwork." *International conference on flexible formwork* (2012): 258-267.
- Oman, Paul. *Chemistry of Epoxies Epoxy Resin, Novolacs, Adducts and Polyurethanes*. PROGRESSIVE EPOXY POLYMERS, INC. New Hampshire, 12 August 2011.
- Peter B. Ramirez, 1954 Meridian Ave., San Jose, Calif. 95125. BUILDING PANEL, MANUFACTURING METHOD AND PANEL ASSEMBLY SYSTEM. United States Patent: Patent 5,519,971. 28 May 1996.
- Pinson, George T. Apparatus for forming sheet metal . USA: Patent US4212188 A. 15 July 1980.
- Portzamparc, Christian de.
<http://www.christiandeportzamparc.com/en/projects/flagship-dior-seoul/>. June 2015.
- Pronk et al., Ir. Arno. "Double curved surafces using a membrane mould." *International Association for Shell and Spatial Structures (IASS)*. Amsterdam, 2015.
- Pronk, et al. *Flexible mould by the use of spring steel mesh*. Amsterdam, 17 August 2015.
- Raun, Kristensen and. "Flexible mat for providing a dynamically reconfigurable double-curved moulding surface in a mould". US: Patent US9168678 B2. 27 October 2015.
- Reinhart et al., Theodore J. *Composites, Engineered Materials Hand Book Volume 1*. Metals Park: ASM Inteernational, 1987.

- Rietbergen, Daan and Karel Jan Vollers. Method and apparatus for forming a double-curved panel from a flat panel. US: Patent US20100147030 A1. 17 June 2010.
- Rogers, S.A. *Dornob*. n.d. 04 November 2016.
- Rooy et al., Van. "Double-curved surfaces using a membrane mould." *Proceedings of the International Association for Shell and Spatial Structures (IASS) Symposium 2009, Valencia*. Ed. Alberto DOMINGO and Carlos LAZARO. Valencia, Spain, 2009.
- Sahba, Fariborz. *Lotus Temple (Bahá'í House of Worship)*. n.d. 18 January 2018. <<https://en.wikiarquitectura.com/building/lotus-temple-bahai-house-of-worship/>>.
- Schipper, Roel. "Shaping building surfaces." *Rumoer Periodical for the building Technologist* 12 October 2015 : 40-45.
- Soderberg, Mark S al, et. Flexible tooling apparatus. USA: Patent US08520446. 03 March 1998.
- "St. Joseph's Hospital." n.d. *Bertrand Goldberg*. 18 January 2018. <<http://bertrandgoldberg.org/projects/st-joseph%E2%80%99s-hospital/>>.
- The Egg. "History & Architecture." n.d. *The Egg*. 18 January 2018. <<http://www.theegg.org/about/historyarchitecture>>.
- Torroja, Eduardo. "Laboratory for Timber Construction." n.d. 18 January 2018. <<https://ibois.epfl.ch/webdav/site/ibois2/shared/torrojaeduardo.pdf>>.
- Webb., William. EXTERIOR WALL PANEL. United States/Bellmore, NY.: Patent 4,852,316. 01 Aug. 1989.
- Wijskamp, Sebastiaan. *Shape distortions in composites forming*. Phd Thesis. The Netherlands: PrintPartners Ipskamp B.V., 2005.

APPENDIX A

Outlier validation:

Double Curve

Test Desc.	C. Agg. (CL)
No. of Outliers	0
Avg.	9.3001226
S.Std. Dev.	7.386
Total No. (n)	40
Tc	3.036

Test ID	Test Value	Tn	Outlier
1	15.60	0.854	No
2	16.02	0.909	No
3	15.87	0.890	No
4	15.68	0.864	No
5	15.46	0.834	No
6	14.74	0.737	No
7	14.74	0.737	No
8	14.71	0.733	No
9	0.67	1.169	No
10	0.32	1.216	No
11	0.15	1.239	No
12	0.00	1.259	No
13	0.00	1.259	No
14	0.21	1.231	No
15	0.71	1.163	No
16	0.67	1.169	No
17	14.74	0.737	No
18	14.92	0.761	No
19	15.11	0.787	No
20	14.88	0.756	No
21	15.10	0.786	No
22	15.11	0.787	No
23	15.41	0.827	No
24	15.09	0.784	No
25	1.00	1.124	No
26	0.37	1.208	No
27	0.21	1.231	No
28	0.00	1.259	No
29	0.00	1.259	No
30	0.00	1.259	No
31	0.64	1.172	No

32	1.16	1.102	No
33	14.88	0.756	No
34	14.80	0.745	No
35	15.44	0.831	No
36	15.21	0.801	No
37	15.13	0.790	No
38	15.10	0.786	No
39	16.09	0.919	No
40	16.05	0.914	No

Concave structure:

Test Desc.	C. Agg. (CL)
No. of Outliers	0
Avg.	17.309524
S.Std. Dev.	8.254
Total No. (n)	35
Tc	2.979

Test ID	Test Value	Tn	Outlier
1	22.00	0.568	No
2	22.67	0.649	No
3	22.67	0.649	No
4	22.33	0.609	No
5	21.33	0.488	No
6	22.00	0.568	No
7	21.33	0.488	No
8	22.33	0.609	No
9	23.00	0.689	No
10	10.67	0.805	No
11	4.33	1.572	No
12	10.00	0.886	No
13	22.67	0.649	No
14	22.67	0.649	No
15	22.67	0.649	No
16	6.67	1.289	No
17	0.33	2.057	No
18	0.00	2.097	No
19	1.33	1.936	No
20	10.67	0.805	No
21	23.33	0.730	No
22	22.00	0.568	No
23	23.00	0.689	No

24	11.83	0.663	No
25	3.00	1.734	No
26	5.33	1.451	No
27	22.67	0.649	No
28	23.33	0.730	No
29	23.00	0.689	No
30	23.33	0.730	No
31	22.67	0.649	No
32	23.00	0.689	No
33	22.00	0.568	No
34	22.33	0.609	No
35	23.33	0.730	No

Convex curve

Test Desc. C. Agg. (CL)
No. of Outliers 0
Avg. 5.8670022
S.Std. Dev. 7.000
Total No. (n) 35
Tc 2.979

Test ID	Test Value	Tn	Outlier
1	0.21	0.808	No
2	0.33	0.790	No
3	0.64	0.747	No
4	0.49	0.769	No
5	0.49	0.769	No
6	0.33	0.790	No
7	0.75	0.731	No
8	0.33	0.790	No
9	4.08	0.255	No
10	16.32	1.493	No
11	15.96	1.442	No
12	16.25	1.483	No
13	3.99	0.268	No
14	0.64	0.746	No
15	1.36	0.643	No
16	15.80	1.419	No
17	15.80	1.419	No
18	15.97	1.443	No
19	15.87	1.429	No
20	15.67	1.401	No
21	0.87	0.714	No
22	0.64	0.747	No
23	4.20	0.239	No
24	16.07	1.458	No

25	15.95	1.440	No
26	15.59	1.389	No
27	4.13	0.248	No
28	0.62	0.749	No
29	0.75	0.731	No
30	1.00	0.695	No
31	1.09	0.682	No
32	0.64	0.747	No
33	0.92	0.706	No
34	0.64	0.746	No
35	0.95	0.702	No

Freeform curve

Test Desc. C. Agg. (CL)

No. of Outliers 0

Avg. 8.5354662

S.Std. Dev. 7.581

Total No. (n) 40

Tc 3.036

Test ID	Test Value	Tn	Outlier
1	15.55	0.925	No
2	0.61	1.046	No
3	16.09	0.996	No
4	0.97	0.998	No
5	15.90	0.972	No
6	6.15	0.315	No
7	16.04	0.990	No
8	0.30	1.086	No
9	0.97	0.998	No
10	16.13	1.002	No
11	0.61	1.046	No
12	15.74	0.950	No
13	0.30	1.086	No
14	16.04	0.990	No
15	0.00	1.126	No
16	14.88	0.837	No
17	15.84	0.964	No
18	0.83	1.016	No
19	16.28	1.021	No
20	0.67	1.038	No

21	16.20	1.011	No
22	1.08	0.983	No
23	16.27	1.021	No
24	0.67	1.038	No
25	1.33	0.950	No
26	16.13	1.002	No
27	0.97	0.998	No
28	16.29	1.022	No
29	1.16	0.973	No
30	16.21	1.013	No
31	0.97	0.998	No
32	16.10	0.998	No
33	15.21	0.881	No
34	0.83	1.016	No
35	16.13	1.002	No
36	1.00	0.994	No
37	16.20	1.011	No
38	1.30	0.954	No
39	16.10	0.998	No
40	1.33	0.950	No

APPENDIX B

Table 5. Double curved height comparison between ideal and actual samples

Actuators		Sample1	Sample2	Sample3	Ideal Geometry	Average	Standard Deviation	Standard Error
Array 1	A1	17	20	21	25.4	19.33	2.08	1.20
	A2	17	21	22	25.4	20.00	2.65	1.53
	A3	16	21	21	25.4	19.33	2.89	1.67
	A4	16	20	21	25.4	19.00	2.65	1.53
	A5	16	20	20	25.4	18.67	2.31	1.33
	A6	16	18.5	18	25.4	17.50	1.32	0.76
	A7	16	18.5	18	25.4	17.50	1.32	0.76
	A8	15	18	18	25.4	17.00	1.73	1.00
Array 2	B1	2	2	2	0	2.00	0.00	0.00
	B2	0.5	0.5	1	0	0.67	0.29	0.17
	B3	0	0	0.5	0	0.17	0.29	0.17
	B4	0	0	0	0	0.00	0.00	0.00
	B5	0	0	0	0	0.00	0.00	0.00
	B6	0.5	0.5	0	0	0.33	0.29	0.17
	B7	1.5	2	2	0	1.83	0.29	0.17
	B8	2	2	2	0	2.00	0.00	0.00
Array 3	C1	17	17	19	25.4	17.67	1.15	0.67
	C2	17.5	19	19	25.4	18.50	0.87	0.50
	C3	18.5	20	19	25.4	19.17	0.76	0.44
	C4	19	19	18	25.4	18.67	0.58	0.33
	C5	19	20	19	25.4	19.33	0.58	0.33
	C6	18.5	20	19	25.4	19.17	0.76	0.44
	C7	19	21	19	25.4	19.67	1.15	0.67
	C8	18.5	20	18	25.4	18.83	1.04	0.60
Array 4	D1	2	3	1	0	2.00	1.00	0.58
	D2	1	1	0.5	0	0.83	0.29	0.17
	D3	0	0.5	0.5	0	0.33	0.29	0.17
	D4	0	0	0	0	0.00	0.00	0.00
	D5	0	0	0	0	0.00	0.00	0.00
	D6	0	0	0	0	0.00	0.00	0.00
	D7	1	2	0.5	0	1.17	0.76	0.44
	D8	3	3	1	0	2.33	1.15	0.67
Array 5	E1	19	19	18	25.4	18.67	0.58	0.33
	E2	19	19	19	25.4	19.00	0.00	0.00
	E3	21	20	20	25.4	20.33	0.58	0.33
	E4	20	19	20	25.4	19.67	0.58	0.33
	E5	18	20	19	25.4	19.00	1.00	0.58
	E6	19	20	19	25.4	19.33	0.58	0.33
	E7	20	23	21	25.4	21.33	1.53	0.88
	E8	19	23	20	25.4	20.67	2.08	1.20

Table 6. Concave Curve height comparison between ideal and actual samples

Actuators		Sample1	Sample2	Sample3	Ideal Geometry	Average	Standard Deviation	Standard Error
Array 1	A1	21	20	25	25.4	22.00	2.65	1.53
	A2	21	22	25	25.4	22.67	2.08	1.20
	A3	20	25	23	25.4	22.67	2.52	1.45
	A4	20	25	22	25.4	22.33	2.52	1.45
	A5	20	24	20	25.4	21.33	2.31	1.33
	A6	22	24	20	25.4	22.00	2.00	1.15
	A7	22	25	17	25.4	21.33	4.04	2.33
Array 2	B1	21	21	25	25.4	22.33	2.31	1.33
	B2	21	23	25	25.4	23.00	2.00	1.15
	B3	11	9	12	0	10.67	1.53	0.88
	B4	5	4	4	0	4.33	0.58	0.33
	B5	10	10	10	0	10.00	0.00	0.00
	B6	22	24	22	25.4	22.67	1.15	0.67
	B7	23	25	20	25.4	22.67	2.52	1.45
Array 3	C1	21	23	24	25.4	22.67	1.53	0.88
	C2	5	8	7	0	6.67	1.53	0.88
	C3	0	0	1	0	0.33	0.58	0.33
	C4	0	0	0	0	0.00	0.00	0.00
	C5	0	3	1	0	1.33	1.53	0.88
	C6	10	12	10	0	10.67	1.15	0.67
	C7	24	24	22	25.4	23.33	1.15	0.67
Array 4	D1	22	19	25	25.4	22.00	3.00	1.73
	D2	23	22	24	25.4	23.00	1.00	0.58
	D3	10	12.5	13	0	11.83	1.61	0.93
	D4	2	3	4	0	3.00	1.00	0.58
	D5	2	6	8	0	5.33	3.06	1.76
	D6	22	22	24	25.4	22.67	1.15	0.67
	D7	24	22	24	25.4	23.33	1.15	0.67
Array 5	E1	24	20	25	25.4	23.00	2.65	1.53
	E2	25	20	25	25.4	23.33	2.89	1.67
	E3	20	23	25	25.4	22.67	2.52	1.45
	E4	21	23	25	25.4	23.00	2.00	1.15
	E5	20	21	25	25.4	22.00	2.65	1.53
	E6	22	20	25	25.4	22.33	2.52	1.45
	E7	24	21	25	25.4	23.33	2.08	1.20

Table 7. Convex curve height comparison between ideal and actual samples

Actuators	Sample1	Sample2	Sample3	Ideal Geometry	Average	Standard Deviation	Standard Error
-----------	---------	---------	---------	----------------	---------	--------------------	----------------

Array 1	A1	0	0.5	0.5	0	0.33	0.29	0.17
	A2	0.5	0	1	0	0.50	0.50	0.29
	A3	2	1	1	0	1.33	0.58	0.33
	A4	1	1	1.5	0	1.17	0.29	0.17
	A5	1.5	1	1	0	1.17	0.29	0.17
	A6	0.5	0	1	0	0.50	0.50	0.29
	A7	1	2	2	0	1.67	0.58	0.33
Array 2	B1	1	1	1	0	1.00	0.00	0.00
	B2	12	11	12	0	11.67	0.58	0.33
	B3	23	22.5	19.5	25.4	21.67	1.89	1.09
	B4	22	22	20	25.4	21.33	1.15	0.67
	B5	22.5	22.5	19	25.4	21.33	2.02	1.17
	B6	11	7	11	0	9.67	2.31	1.33
	B7	0.5	2	1	0	1.17	0.76	0.44
Array 3	C1	4	1.5	3	0	2.83	1.26	0.73
	C2	22	22	22	25.4	22.00	0.00	0.00
	C3	22	21	20	25.4	21.00	1.00	0.58
	C4	22.5	21.5	20.5	25.4	21.50	1.00	0.58
	C5	22	21.5	20	25.4	21.17	1.04	0.60
	C6	21.5	21.5	21	25.4	21.33	0.29	0.17
	C7	1	2.5	2	0	1.83	0.76	0.44
Array 4	D1	2	1	1	0	1.33	0.58	0.33
	D2	12.5	5	9	0	8.83	3.75	2.17
	D3	22.5	22	20	25.4	21.50	1.32	0.76
	D4	22	21.5	19	25.4	20.83	1.61	0.93
	D5	21	21	19.5	25.4	20.50	0.87	0.50
	D6	12	6	10	0	9.33	3.06	1.76
	D7	0.5	2	0.5	0	1.00	0.87	0.50
Array 5	E1	1	2	2	0	1.67	0.58	0.33
	E2	1	3	2	0	2.00	1.00	0.58
	E3	1	3.5	1	0	1.83	1.44	0.83
	E4	1	2	1	0	1.33	0.58	0.33
	E5	0.5	3	0	0	1.17	1.61	0.93
	E6	0.5	2	1	0	1.17	0.76	0.44
	E7	0	3	1	0	1.33	1.53	0.88

Table 8. Freeform Curve height comparison between ideal and actual samples

Actuators		Sample1	Sample2	Sample3	Ideal Geometry	Average	Standard Deviation
Array 1	A1	20	21	21	25.4	20.67	0.58
	A2	0	0	2	0	0.67	1.15

	A3	21	20	23	25.4	21.33	1.53
	A4	3	2	2	0	2.33	0.58
	A5	22.5	20	19	25.4	20.50	1.80
	A6	3	20	2	0	8.33	10.12
	A7	23	20	20	25.4	21.00	1.73
	A8	0	0	1	0	0.33	0.58
Array 2	B1	2	2	3	0	2.33	0.58
	B2	23	22	21	25.4	22.00	1.00
	B3	0	2	0	0	0.67	1.15
	B4	22	20	20	25.4	20.67	1.15
	B5	0	0	1	0	0.33	0.58
	B6	23	20	20	25.4	21.00	1.73
	B7	0	0	0	0	0.00	0.00
	B8	19	19	18	25.4	18.67	0.58
Array 3	C1	22	21.5	22	25.4	21.83	0.29
	C2	0	2	2	0	1.33	1.15
	C3	23.5	22	22.5	25.4	22.67	0.76
	C4	2	2	2	0	2.00	0.00
	C5	23	20	22	25.4	21.67	1.53
	C6	3	2	3	0	2.67	0.58
	C7	23.5	21	22	25.4	22.17	1.26
	C8	0	1	2	0	1.00	1.00
Array 4	D1	4	3	3.5	0	3.50	0.50
	D2	23	23	23	25.4	23.00	0.00
	D3	2	2	3	0	2.33	0.58
	D4	23.5	23	23	25.4	23.17	0.29
	D5	3	1	3	0	2.33	1.15
	D6	23	22	23	25.4	22.67	0.58
	D7	3	2	2	0	2.33	0.58
	D8	22	23	22	25.4	22.33	0.58
Array 5	E1	20	19	20	25.4	19.67	0.58
	E2	0	2	2	0	1.33	1.15
	E3	21	23	22	25.4	22.00	1.00
	E4	1	2	3	0	2.00	1.00
	E5	21	23	22.5	25.4	22.17	1.04
	E6	4	3	3	0	3.33	0.58
	E7	22	23	22	25.4	22.33	0.58
	E8	4	3	3.5	0	3.50	0.50

APPENDIX C

DOUBLE CURVE GEOMETRY VALUES COMPARESSION BETWEEN

DIFFERENT SAMPLES

Anova: Single Factor

SUMMARY

<i>Groups</i>	<i>Count</i>	<i>Sum</i>	<i>Average</i>	<i>Variance</i>
Column 1	40	444.5	11.1125	73.92933
Column 2	40	492.5	12.3125	88.59856
Column 3	40	476	11.9	86.98974

ANOVA

<i>Source of Variation</i>	<i>SS</i>	<i>df</i>	<i>MS</i>	<i>F</i>	<i>P-value</i>	<i>F crit</i>
Between Groups	29.7375	2	14.86875	0.17877	0.836526	3.0737629
Within Groups	9731.188	117	83.17254274			
Total	9760.925	119				

CONCAVE CURVE GEOMETERY VALUES COMPARESSION BETWEEN

DIFFERENT SAMPLES

Anova: Single Factor

SUMMARY

<i>Groups</i>	<i>Count</i>	<i>Sum</i>	<i>Average</i>	<i>Variance</i>
Column 1	35	580	16.5714	70.7226890
Column 2	35	605.5	17.3	67.0617647
Column 3	35	632	18.0571	74.1731092

ANOVA

<i>Source of Variation</i>	<i>SS</i>	<i>df</i>	<i>MS</i>	<i>F</i>	<i>P-value</i>	<i>F crit</i>
Between Groups	38.6333	3	19.3166	0.27340378	0.76134128	3.08546
Within Groups	7206.55	102	70.6525	5	4	5

Total	7245.19	104
-------	---------	-----

CONVEX CURVE GEOMETRY VALUES COMPARESSION BETWEEN
DIFFERENT SAMPLES

Anova: Single Factor

SUMMARY

<i>Groups</i>	<i>Count</i>	<i>Sum</i>	<i>Average</i>	<i>Variance</i>
Column 1	35	311	8.8857143	94.36891
Column 2	35	302	8.6285714	85.22563
Column 3	35	287	8.2	75.26765

ANOVA

<i>Source of Variation</i>	<i>SS</i>	<i>df</i>	<i>MS</i>	<i>F</i>	<i>P-value</i>	<i>F crit</i>
Between Groups	8.4	2	4.2	0.049438	0.9517865	3.085465
Within Groups	8665.314	102	84.954062			
Total	8673.714	104				

FREEFORM CURVE GEOMETRY VALUES COMPARESSION BETWEEN
DIFFERENT SAMPLES

Anova: Single Factor

SUMMARY

<i>Groups</i>	<i>Count</i>	<i>Sum</i>	<i>Average</i>	<i>Variance</i>
Column 1	40	475	11.875	108.266025
Column 2	40	476	11.9125	99.6139423
Column 3	40	471	11.775	96.5634615

ANOVA

<i>Source of Variation</i>	<i>SS</i>	<i>df</i>	<i>MS</i>	<i>F</i>	<i>P-value</i>	<i>F crit</i>
Between Groups	0.40416	2	0.202083	0.00199133	0.99801067	3.07376
Within Groups	11873.2	117	101.4811	9	6	3
Total	11873.7	119				

APPENDIX D

DOUBLE CURVE GEOMETRY VALUES COMPERSION BETWEEN IDEAL GEOMETRY VS ACTUAL SAMPLE

Anova: Single
Factor

SUMMARY

<i>Groups</i>	<i>Count</i>	<i>Sum</i>	<i>Average</i>	<i>Variance</i>
Column 1	40	609.6	15.24	158.8086
Column 2	40	471	11.775	82.44808

ANOVA

<i>Source of Variation</i>	<i>SS</i>	<i>df</i>	<i>MS</i>	<i>F</i>	<i>P-value</i>	<i>F crit</i>
Between Groups	240.1245	1	240.1245	1.990614	0.162253	3.963472
Within Groups	9409.011	78	120.62835			
Total	9649.136	79				

CONCAVE CURVE GEOMETRY VALUES COMPERSION BETWEEN IDEAL GEOMETRY VS ACTUAL SAMPLE

Anova: Single Factor

SUMMARY

<i>Groups</i>	<i>Count</i>	<i>Sum</i>	<i>Average</i>	<i>Variance</i>
Column 1	35	605.833	17.3095	68.1244164
Column 2	35	609.6	17.4171	143.127932

ANOVA

<i>Source of Variation</i>	<i>SS</i>	<i>df</i>	<i>MS</i>	<i>F</i>	<i>P-value</i>	<i>F crit</i>
Between Groups	0.20268	3	0.20268	0.00191886	0.96518832	3.981896
Within Groups	7182.58	68	105.626	7	5	3

	7182.78		
Total	3	69	

CONVEX CURVE GEOMETRY VALUES COMPERSION BETWEEN IDEAL
GEOMETRY VS ACTUAL SAMPLE

Anova: Single Factor

SUMMARY

<i>Groups</i>	<i>Count</i>	<i>Sum</i>	<i>Average</i>	<i>Variance</i>
Column 1	35	279.4	7.982857	143.1279
Column 2	35	300	8.571429	83.8436

ANOVA

<i>Source of Variation</i>	<i>SS</i>	<i>df</i>	<i>MS</i>	<i>F</i>	<i>P-value</i>	<i>F crit</i>
Between Groups	6.062286	1	6.062286	0.053419	0.817911	3.981896
Within Groups	7717.032	68	113.4858			
Total	7723.095	69				

FREEFORM CURVE GEOMETRY VALUES COMPERSION BETWEEN IDEAL
GEOMETRY VS ACTUAL SAMPLE

Anova: Single
Factor

SUMMARY

<i>Groups</i>	<i>Count</i>	<i>Sum</i>	<i>Average</i>	<i>Variance</i>
Column 1	40	508	12.7	165.4256
Column 2	40	474.1667	11.85417	99.14557

ANOVA

<i>Source of Variation</i>	<i>SS</i>	<i>df</i>	<i>MS</i>	<i>F</i>	<i>P-value</i>	<i>F crit</i>
Between Groups	14.30868056	1	14.30868	0.108165	0.743124	3.963472
Within Groups	10318.27708	78	132.2856			
Total	10332.58576	79				

APPENDIX E

DESCRIPTIVE STATISTICS DOUBLE COVERED

<i>Column1 Higher Value</i>		<i>Column2 Lower Value</i>	
Mean	19.0555556	Mean	0.854167
Standard Error	0.20502608	Standard Error	0.222504
Median	19.0833333	Median	0.5
Mode	19.3333333	Mode	0
Standard Deviation	1.00441858	Standard Deviation	0.890017
Sample Variance	1.00885668	Sample Variance	0.79213
			-
Kurtosis	0.49674436	Kurtosis	1.498385
Skewness	0.01035354	Skewness	0.539132
Range	4.3333333	Range	2.333333
Minimum	17	Minimum	0
Maximum	21.3333333	Maximum	2.333333
Sum	457.333333	Sum	13.66667
Count	24	Count	16
Largest(1)	21.3333333	Largest(1)	2.333333
Smallest(1)	17	Smallest(1)	0
Confidence		Confidence	
Level(95.0%)	0.42412877	Level(95.0%)	0.474256

DESCRIPTIVE STATISTICS CONCAVE CURVE

<i>Column1 Higher Value</i>		<i>Column2 Lower Value</i>	
Mean	22.28	Mean	6.19697
Standard Error	0.219	Standard Error	1.338403
Median	22.67	Median	7.333333
Mode	22.67	Mode	10.66667
Standard Deviation	1.071	Standard Deviation	4.43898
Sample Variance	1.147	Sample Variance	19.70455
Kurtosis	3.346	Kurtosis	-1.66486
Skewness	-1.8	Skewness	-0.21983
Range	4	Range	11.83333
Minimum	19.33	Minimum	0
Maximum	23.33	Maximum	11.83333
Sum	534.7	Sum	68.16667
Count	24	Count	11
Largest(1)	23.33	Largest(1)	11.83333
Smallest(1)	19.33	Smallest(1)	0

Confidence
Level(95.0%) 0.452

Confidence
Level(95.0%) 2.982147

DESCRIPTIVE STATISTICS CONVEX CURVE

<i>Column1 Higher Value</i>	
Mean	21.288
Standard Error	0.1233
Median	21.333
Mode	21.333
Standard Deviation	0.4089
Sample Variance	0.1672
Kurtosis	0.5365
Skewness	-0.311
Range	1.5
Minimum	20.5
Maximum	22
Sum	234.17
Count	11
Largest(1)	22
Smallest(1)	20.5
Confidence Level(95.0%)	0.2747

<i>Column2 Lower Value</i>	
Mean	2.7430556
Standard Error	0.6795982
Median	1.3333333
Mode	1.1666667
Standard Deviation	3.3293379
Sample Variance	11.084491
Kurtosis	2.1049859
Skewness	1.892213
Range	11.333333
Minimum	0.3333333
Maximum	11.666667
Sum	65.833333
Count	24
Largest(1)	11.666667
Smallest(1)	0.3333333
Confidence Level(95.0%)	1.4058561

DESCRIPTIVE STATISTICS FREEFORM CURVE

<i>Column1 Higher Value</i>	
Mean	21.575
Standard Error	0.255774
Median	21.91667
Mode	20.66667
Standard Deviation	1.143856
Sample Variance	1.308406
Kurtosis	0.768501
Skewness	-0.92602
Range	4.5
Minimum	18.66667
Maximum	23.16667
Sum	431.5
Count	20
Largest(1)	23.16667
Smallest(1)	18.66667
Confidence Level(95.0%)	0.535341

<i>Column2 Lower Value</i>	
Mean	2.133333
Standard Error	0.404037
Median	2.166667
Mode	2.333333
Standard Deviation	1.806907
Sample Variance	3.264912
Kurtosis	6.898605
Skewness	2.133093
Range	8.333333
Minimum	0
Maximum	8.333333
Sum	42.66667
Count	20
Largest(1)	8.333333
Smallest(1)	0
Confidence Level(95.0%)	0.845658

